

Generalised global symmetries and magnetohydrodynamic waves in a strongly interacting holographic plasma

Sašo Grozdanov^{*} and Napat Poovuttikul[†]

*Instituut-Lorentz for Theoretical Physics,
Leiden University, Niels Bohrweg 2,
Leiden 2333 CA, The Netherlands*

Abstract

We begin the exploration of magnetohydrodynamics (MHD) in strongly coupled plasmas by constructing and analysing a holographic dual to a recent, generalised global symmetry-based formulation of dissipative MHD. The simplest holographic dual to the effective theory of MHD that was proposed as a description of plasmas with any equation of state and transport coefficients contains dynamical graviton and two-form gauge field fluctuations in a magnetised black brane background. The dual field theory, which is closely related to the large- N_c , $\mathcal{N} = 4$ supersymmetric Yang-Mills theory at (infinitely) strong coupling, is, as we argue, in our setup coupled to a dynamical $U(1)$ gauge field with a renormalisation condition-dependent electromagnetic coupling. After constructing the holographic dictionary, we compute the dual equation of state and transport coefficients, and for the first time analyse phenomenology of MHD waves in a strongly interacting, dense plasma with a (holographic) microscopic description. From weak to extremely strong magnetic fields, several predictions for the behaviour of Alfvén and magnetosonic waves are discussed.

arXiv:1707.04182v1 [hep-th] 13 Jul 2017

^{*} grozdanov@lorentz.leidenuniv.nl

[†] poovuttikul@lorentz.leidenuniv.nl

CONTENTS

I. Introduction	2
II. Matter coupled to electromagnetic interactions	6
A. Quantum electrodynamics	6
B. Strongly interacting holographic matter coupled to dynamical electromagnetism	8
III. Holographic analysis: equation of state and transport coefficients	11
A. Holographic action and the magnetic brane	12
B. Holographic renormalisation and the bulk/boundary dictionary	14
C. Equation of state	17
D. Transport coefficients	20
IV. Magnetohydrodynamic waves in a strongly coupled plasma	25
A. Speeds and attenuations of MHD waves	29
B. MHD modes on a complex frequency plane	30
C. Electric charge dependence	33
V. Discussion	35
Acknowledgments	37
A. Kubo formulae for first-order transport coefficients	38
B. Further details regarding the derivation of the transport coefficients	39
C. Dispersion relations of magnetosonic waves	43
References	45

I. INTRODUCTION

Magnetohydrodynamics (MHD) is a hydrodynamic theory of long-range excitations in plasmas (ionised gases) (see e.g. [1, 2]), which has been applied to systems ranging from the physics of fusion reactors to astrophysical objects. In the modern language of hydrodynamics formulated as an effective field theory [3–17], MHD should describe the dynamics of infrared (IR) charge-neutral states in terms of massless effective degrees of freedom. These plasma ground states are characterised by an equation of state with a finite magnetic field. On the other hand, the electric field is suppressed due to the screening of electromagnetic interactions and is only induced on shorter length scales than the (thermodynamic) size of the system. In their standard form, the equations of motion that describe the evolution of plasmas are formulated as a combination of macroscopic fluid equations (continuity equation and the non-dissipative Euler, or dissipative

Navier-Stokes equation), coupled to the microscopic electromagnetic Maxwell's equations. In ideal, non-dissipative form, the set of dynamical equations is

$$\partial_t \rho + \vec{\nabla} \cdot (\rho \vec{v}) = 0, \quad (1)$$

$$\rho (\partial_t + \vec{v} \cdot \nabla) \vec{v} = -\vec{\nabla} p + \vec{J} \times \vec{B}, \quad (2)$$

$$\partial_t \vec{B} = \vec{\nabla} \times (\vec{v} \times \vec{B}), \quad (3)$$

$$(\partial_t + \vec{v} \cdot \nabla) \left(\frac{p}{\rho^\gamma} \right) = 0. \quad (4)$$

The magnetic field is constrained by

$$\vec{\nabla} \cdot \vec{B} = 0. \quad (5)$$

Eq. (1) is the continuity equation and Eq. (2) the Euler equation in the presence of the Lorentz force $\vec{J} \times \vec{B}$, with \vec{J} given by the low-frequency limit of the Ampere's law ($\partial_t \vec{E} \rightarrow 0$)

$$\vec{J} = \frac{1}{\mu_0} \vec{\nabla} \times \vec{B}. \quad (6)$$

Eq. (3) is the Faraday's induction law with the electric field fixed by the assumption of the ideal Ohm's law

$$\vec{E} + \vec{v} \times \vec{B} = 0, \quad (7)$$

which is derived by taking the conductivity in the (Lorentz transformed) Ohm's law $\vec{J}/\sigma = \vec{E} + \vec{v} \times \vec{B}$ to infinity, i.e. $\sigma \rightarrow \infty$. The constraint equation (5) is the magnetic Gauss's law. Since the ideal Ohm's law completely fixes \vec{E} , the electric Gauss's law plays no role in the equations of MHD. Eq. (4) is the adiabatic equation of state relating density and pressure. Usually, one takes $\gamma = 5/3$. Altogether, Eqs. (1)–(4) give eight dynamical equations for eight unknown functions ρ , p , \vec{v} and \vec{B} , subject to the magnetic field constraint (5).

While the above equations are closed, solvable and have been successfully applied to a variety of phenomena in plasma physics, they are only applicable within the specific assumptions used to construct them. This means that they are only valid for electromagnetism controlled by Maxwell's equations in the limit of ideal Ohm's law (no possibility of strong-field pair production, etc.) and for the specific equation of state in Eq. (4). This equation of state encodes a separation between the fluid and the charge carrying sectors, for which the justification, beyond assuming weakly coupled Maxwell electromagnetism, also assumes very weak interactions between the fluid degrees of freedom and electromagnetism inside the plasma. Concretely, the latter statement is reflected in the equation of state permitting no dependence on the magnetic properties controlled by the charged sector. Furthermore, because of a lack of a symmetry principle behind the construction of ideal MHD, these equations are difficult to extend unambiguously to the most general, higher-order, dissipative theory in the gradient expansion (the Knudsen number expansion) [18–21].¹ As

¹ We note that in standard MHD, as formulated in Eqs. (1)–(4), only the fluid sector has a well-defined and finite Knudsen number.

such, the traditional formulation of MHD lacks generality and cannot be compatible with a variety of IR effective theories of plasmas that could (in principle) be derived from quantum field theory, in particular, in the presence of a strong magnetic field.

These issues were addressed in a recent work [22], where MHD was formulated by following the effective field theory philosophy behind the construction of relativistic hydrodynamics (see e.g. [21, 23]). Namely, MHD was formulated by only considering global conserved operators and writing them in terms of the most general hydrodynamic gradient expansion of the IR hydrodynamic fields [22].² With such an expansion in hand, conservation equations then completely determine the temporal dynamics of a plasma with any equation of state. As in hydrodynamics, all of the details of the equation of state and transport coefficients are left to be determined by the microscopics of the underlying theory.

The two relevant global symmetries describing the long-range dynamics of a plasma were argued to give the stress-energy tensor $T^{\mu\nu}$ and a conserved anti-symmetric two-form current $J^{\mu\nu}$ [22]:

$$\nabla_\mu T^{\mu\nu} = H^\nu{}_{\mu\sigma} J^{\mu\sigma}, \quad (8)$$

$$\nabla_\mu J^{\mu\nu} = 0. \quad (9)$$

While $T^{\mu\nu}$ corresponds to conserved energy-momentum, $J^{\mu\nu}$ is the manifestation of a generalised global $U(1)$ symmetry, which can be sourced (and gauged) by a two-form gauge field $b_{\mu\nu}$ [31]. $H^\nu{}_{\mu\sigma}$ is a three-form field strength that can be turned on by an external two-form gauge field, $H = db_{ext}$. This generalised global symmetry is a consequence of the absence of magnetic monopoles and directly corresponds to the conserved number of magnetic flux lines crossing a co-dimension two surface (in a four dimensional plasma). Normally, it is expressed in terms of the (topological) Bianchi identity

$$dF = 0, \quad (10)$$

where $F = dA$ and A is the abelian electromagnetic field. In the language of a two-form current used in Eq. (9),

$$J^{\mu\nu} = \frac{1}{2} \epsilon^{\mu\nu\rho\sigma} F_{\rho\sigma}. \quad (11)$$

Eqs. (8) and (9) give seven dynamical equations of motion (and one constraint). To solve the equations, we introduce the following hydrodynamical fields: a velocity field u^μ , a temperature field T , a chemical potential μ that corresponds to the density of magnetic flux lines and a vector h^μ , which can be thought as a hydrodynamical realisation of a fluctuating magnetic field. The vectors are normalised as $u_\mu u^\mu = -1$, $h_\mu h^\mu = 1$, $u_\mu h^\mu = 0$, together resulting in $10 - 3 = 7$ degrees of freedom. A (directed) velocity flow of the plasma breaks the Lorentz symmetry from $SO(3, 1)$ to $SO(3)$, which is further broken by the additional vector (magnetic field) to $SO(2)$.³ The projector transverse to both u^μ and h^μ is defined as $\Delta^{\mu\nu} = g^{\mu\nu} - u^\mu u^\nu - h^\mu h^\nu$ and has a trace $\Delta^\mu{}_\mu = 2$.

² See also [24] and Ref. [25], which includes a valuable comparison of various related past works, such as [26–28].

For a new treatment of charged fluids in an external electromagnetic field, see [25, 29]. Of further interest is also a recently proposed field theory description of polarised fluids [30].

³ Note that at zero temperature, in a plasma with a non-fluctuating temperature field, the symmetry is enhanced to $SO(1, 1) \times SO(2)$ [22].

The constitutive relations for the conserved tensors with a positive local entropy production [15] and charge conjugation symmetry can now be expanded to first order in derivatives as [22]

$$T^{\mu\nu} = (\varepsilon + p) u^\mu u^\nu + p g^{\mu\nu} - \mu\rho h^\mu h^\nu + \delta f \Delta^{\mu\nu} + \delta\tau h^\mu h^\nu + 2\ell^{(\mu} h^{\nu)} + t^{\mu\nu}, \quad (12)$$

$$J^{\mu\nu} = 2\rho u^{[\mu} h^{\nu]} + 2m^{[\mu} h^{\nu]} + s^{\mu\nu}, \quad (13)$$

where

$$\delta f = -\zeta_\perp \Delta^{\mu\nu} \nabla_\mu u_\nu - \zeta_\times^{(1)} h^\mu h^\nu \nabla_\mu u_\nu, \quad (14)$$

$$\delta\tau = -\zeta_\times^{(2)} \Delta^{\mu\nu} \nabla_\mu u_\nu - 2\zeta_\parallel h^\mu h^\nu \nabla_\mu u_\nu, \quad (15)$$

$$\ell^\mu = -2\eta_\parallel \Delta^{\mu\sigma} h^\nu \nabla_{(\sigma} u_{\nu)}, \quad (16)$$

$$t^{\mu\nu} = -2\eta_\perp \left(\Delta^{\mu\rho} \Delta^{\nu\sigma} - \frac{1}{2} \Delta^{\mu\nu} \Delta^{\rho\sigma} \right) \nabla_{(\rho} u_{\sigma)}, \quad (17)$$

$$m^\mu = -2r_\perp \Delta^{\mu\beta} h^\nu \left(T \nabla_{[\beta} \left(\frac{h_{\nu]}^\mu}{T} \right) + u_\sigma H^\sigma_{\beta\nu} \right), \quad (18)$$

$$s^{\mu\nu} = -2r_\parallel \Delta^{\mu\rho} \Delta^{\nu\sigma} \left(\mu \nabla_{[\rho} h_{\sigma]} + u_\lambda H^\lambda_{\rho\sigma} \right). \quad (19)$$

The thermodynamic relations between ε , p and ρ , which need to be obeyed by the equation of state $p(T, \mu)$ are

$$\varepsilon + p = sT + \mu\rho, \quad (20)$$

$$dp = s dT + \rho d\mu. \quad (21)$$

Furthermore, for the theory to be invariant under time-reversal, the Onsager relation implies that $\zeta_\times^{(1)} = \zeta_\times^{(2)} \equiv \zeta_\times$. Thus, first-order dissipative corrections to ideal MHD are controlled by seven transport coefficients: η_\perp , η_\parallel , ζ_\perp , ζ_\parallel , ζ_\times , r_\perp and r_\parallel . Each one can be computed from a set of Kubo formulae presented in [22, 25] and reviewed in Appendix A. The transport coefficients should obey the following positive entropy production constraints: $\eta_\perp \geq 0$, $\eta_\parallel \geq 0$, $r_\perp \geq 0$, $r_\parallel \geq 0$, $\zeta_\perp \geq 0$ and $\zeta_\perp \zeta_\parallel \geq \zeta_\times^2$. In absence of charge conjugation symmetry, the theory has four additional transport coefficients, resulting in total in eleven transport coefficients [25]. The precise connection between the above formalism of MHD using the concept of generalised global symmetries and MHD expressed in terms of electromagnetic fields, which match in the limit of a small magnetic field (compared to the temperature of the plasma), was established in Ref. [25].

Since the effective theory [22] makes no assumption regarding the microscopic details of the plasma, then, should such details somehow be computable from quantum field theory, or otherwise, the effective MHD can be used in solar plasma physics, fusion reactor physics, astrophysical plasma physics and even QCD quark-gluon plasma resulting from nuclear collisions. Of course, computing the microscopic properties of such systems is extremely difficult. In this work, we will resort to using holographic duality. By using standard holographic methods applicable to hydrodynamics [32–34], our analysis will provide us with the required microscopic data of a strongly interacting toy model plasma needed to describe the phenomenology of MHD waves.

The paper is structured as follows: first, in Section II, we review important aspects of gauge theories with a matter sector coupled to dynamical $U(1)$, which can describe a plasma in the IR

limit. In particular, we focus on the discussion of how to couple a strongly interacting field theory with a holographic dual to dynamical electromagnetism, all within a holographic setup. Then, in Section III, we explore this holographic setup in detail, develop the holographic dictionary and use it to compute the microscopic properties of the dual plasma, i.e. the equation of state and first-order transport coefficients. In Section IV, we then use this data to analyse the phenomenology of propagating MHD modes—Alfvén and magnetosonic waves. Finally, we conclude with a discussion and a summary of the most important findings in Section V. Three appendices are devoted to a derivation of the relevant Kubo formulae (Appendix A), details regarding the derivation of horizon formulae for the transport coefficients (Appendix B) and a derivation of the magnetosonic dispersion relations (Appendix C).

Note added: We note that in addition to this paper on the holographic dual of MHD from the perspective of generalised global symmetries, a closely related work, i.e. Ref. [35], also studies various aspects of generalised global symmetries in gauge-gravity duality and holographic dual(s) of [22]. Although the two concurrent and complementary papers focus on different aspects of holography, there is overlap between our Sections II B and III and parts of Ref. [35].

II. MATTER COUPLED TO ELECTROMAGNETIC INTERACTIONS

A microscopic theory from which an effective description of a plasma can arise comprises of a matter sector that interacts through an electromagnetic $U(1)$ gauge field. The simplest example of such a theory is quantum electrodynamics. In other theories, the matter sector may itself exhibit complicated physics with additional gauge interactions, such as in QCD. In this work, the theory that we will study contains an infinitely strongly coupled holographic matter sector (closely related to $\mathcal{N} = 4$ supersymmetric $SU(N_c)$ Yang-Mills) with infinite N_c . Because of the coupling between matter and dynamical electromagnetism, the holographic setup and the interpretation of results is somewhat subtle. For this reason, we begin our discussion by reviewing some relevant aspects of quantum field theory in a line of arguments similar to [36].

A. Quantum electrodynamics

The simplest example of a theory coupling matter to electromagnetism is quantum electrodynamics (QED). QED is a $U(1)$ gauge theory that contains a (massive) Dirac fermion ψ (describing electrons and positrons) and a massless photon field A_μ .⁴

$$S_{QED} = - \int d^4x \left[i\bar{\psi}\gamma^\mu D_\mu\psi + m\bar{\psi}\psi + \frac{1}{4e^2}F_{\mu\nu}F^{\mu\nu} \right]. \quad (22)$$

D_μ is the gauge covariant derivative that couples A_μ to the fermion current (with the coupling e scaled out from the interaction). For a detailed discussion of various properties of QED, see e.g. [37–39].

⁴ We use the mostly positive convention for the metric tensor, so that $\eta_{\mu\nu} = \{-1, +1, +1, +1\}$.

The stress-energy tensor of the theory is

$$T^{\mu\nu} = \frac{1}{2}\bar{\psi}i(\gamma^\mu D^\nu + \gamma^\nu D^\mu)\psi - \eta^{\mu\nu}\bar{\psi}(i\gamma^\mu D_\mu + m)\psi + \frac{1}{e^2}\left[F^{\mu\lambda}F^\nu{}_\lambda - \frac{1}{4}\eta^{\mu\nu}F^{\rho\sigma}F_{\rho\sigma}\right]. \quad (23)$$

In the massless limit ($m = 0$), the theory is classically scale invariant, which is reflected in the vanishing trace of the stress-energy tensor, $T^\mu{}_\mu = 0$. Quantum mechanically, the theory does not remain scale invariant. The trace receives a correction proportional to the beta function of the electromagnetic coupling,

$$T^\mu{}_\mu = -\frac{\beta(e)}{2e^3}F_{\mu\nu}F^{\mu\nu}. \quad (24)$$

This is the anomalous breaking of scale invariance—the so-called trace anomaly. The running electromagnetic coupling $e(\mu)$ depends on the renormalisation group scale μ . To first order in perturbation theory, the beta function is

$$\beta(e) = \mu\frac{de}{d\mu} = \frac{e^3}{12\pi^2}, \quad (25)$$

which, integrated on the interval $\mu \in [M, \Lambda]$, gives the running coupling

$$\frac{1}{e(\Lambda)^2} = \frac{1}{e(M)^2} - \frac{\ln(\Lambda/M)}{6\pi^2}. \quad (26)$$

Here, M is some IR RG scale at which the electric charge takes the renormalised physical value, $e_r = e(M)$, and Λ is the UV cut-off. Note that at the Landau pole, $\Lambda = \Lambda_{EM}$, the left-hand-side of (26) vanishes. On the other hand, the expectation value of the stress-energy tensor is a physical quantity and therefore cannot depend on μ . This statement is encoded in the following identity, which leads to the Callan-Symanzik equation:

$$\mu\frac{d}{d\mu}\langle T^{\mu\nu}\rangle = 0. \quad (27)$$

Since we are interested in neutral IR plasma states in QED that can be described by an effective theory of MHD, we can consider the (ground state) expectation value of the photon field to produce a non-zero magnetic field and a vanishing (screened) electric field,

$$\langle A_\mu\rangle = \frac{1}{2}\mathcal{B}(x^1\delta^2{}_\mu - x^2\delta^1{}_\mu). \quad (28)$$

\mathcal{B} is the magnitude of the “background” magnetic field pointing in the $x^3 = z$ direction. The IR spectrum of the theory has a gapped-out photon, i.e. long-range charge neutrality, which allows us to neglect quantum fluctuations of A_μ . For such a plasma state, Eq. (24) yields

$$\langle T^\mu{}_\nu\rangle = -\frac{\beta(e)}{e^3}\mathcal{B}^2 = -\frac{1}{12\pi^2}\mathcal{B}^2 + \mathcal{O}(e^2). \quad (29)$$

Furthermore, the expectation value of the stress-energy tensor can be conveniently split into the matter (containing matter-light interactions) and the purely electromagnetic parts,

$$\begin{aligned} \langle T^{\mu\nu}\rangle &= \langle T_{matter}^{\mu\nu}(\mu)\rangle + \frac{1}{e(\mu)^2}\left[F^{\mu\lambda}F^\nu{}_\lambda - \frac{1}{4}\eta^{\mu\nu}F^{\rho\sigma}F_{\rho\sigma}\right] \\ &= \langle T_{matter}^{\mu\nu}(\Lambda/M)\rangle + \left(\frac{1}{e_r^2} - \frac{\ln(\Lambda/M)}{6\pi^2}\right)\frac{\mathcal{B}^2}{2} \times \begin{bmatrix} 1 & 0 & 0 & 0 \\ 0 & 1 & 0 & 0 \\ 0 & 0 & 1 & 0 \\ 0 & 0 & 0 & -1 \end{bmatrix}, \end{aligned} \quad (30)$$

where in the second line, we chose to evaluate the expectation value at the UV cut-off $\mu = \Lambda$. Note that because $\langle T^{\mu\nu} \rangle$ is μ -independent (cf. Eq. (27)), this choice does not influence the final value of $\langle T^{\mu\nu} \rangle$.

B. Strongly interacting holographic matter coupled to dynamical electromagnetism

We now turn our attention to the holographic strongly interacting theory that will be investigated in the remainder of this paper. Throughout our discussion, it will prove useful to think of the matter sector as that of the best understood holographic example—the conformal $\mathcal{N} = 4$ supersymmetric Yang-Mills theory (SYM) with an infinite number of colours N_c and an infinite 't Hooft coupling λ . However, as will become clear below, the theory dual to our holographic setup will not be precisely the $\mathcal{N} = 4$ SYM coupled to a $U(1)$ gauge field, but rather its deformation, of which the microscopic definition will not be investigated in detail. Instead, the model studied here should be considered as a bottom-up construction—the simplest dual of a strongly coupled plasma, which can be described with magnetohydrodynamics in the infrared limit.

The field content of $\mathcal{N} = 4$ SYM are four Weyl fermions, three complex scalars and a vector field, all transforming under the adjoint representation of $SU(N_c)$. The theory also has an $SU(4)_R$ R-symmetry owing to its extended supersymmetry. The adjoint fields together represent the matter content of a hypothetical plasma, which further requires the fields to be (minimally) coupled to an electromagnetic $U(1)$ gauge group (with e the electromagnetic coupling). In $\mathcal{N} = 4$ SYM, this can be achieved by gauging the $U(1)_R$ subgroup of $SU(4)_R$. Under $U(1)_R$, the Weyl fermions transform with the charges $\{+3, -1, -1, -1\}/\sqrt{3}$ and the complex scalars all have charge $+2/\sqrt{3}$ (for details regarding the choice of the normalisation, see [36]). Such a system can be considered as a strongly coupled toy model for a QCD plasma in which the quarks interact with photons as well as with the $SU(3)$ vector gluons.

A crucial fact about $\mathcal{N} = 4$ SYM is that the R -current of $\mathcal{N} = 4$ becomes anomalous in the presence of electromagnetism. For this reason, the $U(1)_R$, which is gauged, is also anomalous and thus the theory has to be deformed in some way to reestablish its self-consistency. As pointed out in [36], one way to do this is by adding a set of spectator fermions that only interact electromagnetically and “absorb” the anomaly. We will assume that the gauge anomaly can be cancelled by some deformation of the theory so that the quantum expectation value of the $U(1)_R$ R-current J_R^μ remains conserved, $\nabla_\mu \langle J_R^\mu \rangle = 0$. We can then write the total bare action of the $SU(N_c) \times U(1)$ gauge theory as

$$S_{plasma} = S_{matter} + \int d^4x A_\mu J_R^\mu - \frac{1}{4e^2} \int d^4x F_{\mu\nu} F^{\mu\nu}, \quad (31)$$

where A_μ is the dynamical electromagnetic gauge field and $F = dA$. The expectation value of the conserved operator J_R^μ contains a trace over the colour index of the adjoint matter field and therefore scales as N_c^2 . Since it is coupled to a single photon, the Maxwell part of the total plasma action S_{plasma} contains no powers of N_c .

As in the QED plasma, we will consider the photons to be gapped out from the IR spectrum

so that A_μ will only produce a (classical) magnetic field

$$\langle A_\mu \rangle = \frac{1}{2} \mathcal{B} (x^1 \delta^2_\mu - x^2 \delta^1_\mu). \quad (32)$$

In order to maintain the neutrality of the plasma, we will set the electric $U(1)_R$ chemical potential to zero, $\mu_R = \langle A_0 \rangle = 0$.⁵ For this reason, the electric one-form (or vector) conserved $U(1)_R$ R-current will play no role in the hydrodynamic IR limit of the theory, so $\langle J_R^\mu \rangle = 0$.

The plasma has a conserved stress-energy tensor to which both the matter (along with its interaction with the electromagnetic field) and the purely electromagnetic sectors contribute,

$$\langle T^{\mu\nu} \rangle = \langle T_{matter}^{\mu\nu}(\Lambda/M) \rangle + \frac{1}{e(\Lambda/M)^2} \left[\langle F^{\mu\lambda} F^\nu{}_\lambda \rangle - \frac{1}{4} \eta^{\mu\nu} \langle F^{\rho\sigma} F_{\rho\sigma} \rangle \right]. \quad (33)$$

The trace of the superconformal theory again experiences an anomaly proportional to the beta function of the electromagnetic coupling (cf. Eq. (29)), which in $\mathcal{N} = 4$ theory turns out to be one-loop exact in the presence of a background electromagnetic field and follows from a special case of the NSVZ beta function (see Refs. [36, 42, 43]),⁶

$$\langle T^\mu{}_\mu \rangle = -\frac{\beta(e)}{e^3} \mathcal{B}^2 = -\frac{N_c^2}{4\pi^2} \mathcal{B}^2. \quad (34)$$

The beta function for the inverse electromagnetic coupling is then

$$\beta(1/e^2) = \mu \frac{de^{-2}}{d\mu} = -\frac{N_c^2}{2\pi^2} \left[\frac{1}{6} \sum_{\alpha=1}^4 (q_f^\alpha)^2 + \frac{1}{12} \sum_{a=1}^3 (q_s^a)^2 \right] = -\frac{N_c^2}{2\pi^2}, \quad (35)$$

with the fermionic and the scalar R-charges being $q_f^\alpha = \{+3, -1, -1, -1\}/\sqrt{3}$ and $q_s^a = \{2, 2, 2\}/\sqrt{3}$, respectively. In analogy with Eq. (26) in QED, by integrating the beta function equation, we find

$$\frac{1}{e^2(\Lambda)} = \frac{1}{e^2(M)} - \frac{N_c^2}{2\pi^2} \ln(\Lambda/M). \quad (36)$$

It is essential to stress that even though our holographic theory will not be exactly dual to the $\mathcal{N} = 4$ SYM theory, it will give us the same trace anomaly and thus the same electromagnetic beta function. Since the NSVZ beta function (35) is only sensitive to the matter content, this match can be interpreted as our working with a theory with the $U(1)$ -gauged matter content and R-charges of $\mathcal{N} = 4$ but with a deformed Lagrangian and possibly additional matter that is ungauged under the $U(1)$.

Beyond the stress-energy tensor of the theory discussed thus far, the only other (generalised) global symmetry of interest to describing a plasma state is the higher-form $U(1)$ symmetry that corresponds to the conserved number of magnetic flux lines crossing a two-surface. The symmetry results in a conserved two-form current $\langle J^{\mu\nu} \rangle \neq 0$ and was discussed in Section I. The generating functional of the field theory that can be used to study MHD of a magnetised plasma in which the two globally conserved operators are $T^{\mu\nu}$ and $J^{\mu\nu}$ is

$$W[g_{\mu\nu}, b_{\mu\nu}] = \left\langle \exp \left[i \int d^4x \sqrt{-g} \left(\frac{1}{2} T^{\mu\nu} g_{\mu\nu} + J^{\mu\nu} b_{\mu\nu} \right) \right] \right\rangle. \quad (37)$$

⁵ For a discussion of supersymmetric gauge theories with non-zero R-charge densities, see e.g. [40, 41]

⁶ Note that as $N_c \rightarrow \infty$, $N_c^2 - 1 \approx N_c^2$.

The simplest holographic dual of such a state is one that contains a five-dimensional bulk with a dynamical graviton (metric tensor G_{ab}) described by the Einstein-Hilbert action, a negative cosmological constant and a two-form bulk gauge field B_{ab} :⁷

$$S = \frac{1}{2\kappa_5^2} \int d^5x \sqrt{-G} \left(R + \frac{12}{L^2} - \frac{1}{3e_H^2} H_{abc} H^{abc} \right). \quad (38)$$

In standard (Dirichlet) quantisation, the two fields asymptote to $g_{\mu\nu}$ and $b_{\mu\nu}$ at the boundary and source $T^{\mu\nu}$ and $J^{\mu\nu}$. Furthermore, H is the three-form defined as $H = dB$. In component notation, $B = \frac{1}{2} B_{ab} dx^a \wedge dx^b$ and $H = \frac{1}{6} H_{abc} dx^a \wedge dx^b \wedge dx^c$. The two-form gauge field action is the bulk Maxwell Lagrangian $F \wedge \star F$ written in terms of the five-dimensional Hodge dual three-form $H = \star F$, giving the Lagrangian term $H \wedge \star H$. In most of our work, we will set $e_H = L = 1$. Because the two bulk theories are related by dualisation, the background solution to the equations of motion derived from (38) give rise to the same magnetised black brane solution known from the Einstein-Maxwell theory [44].

In the absence of the two-form term, the action (38) arises from a consistent truncation of type IIB string theory on S^5 and is upon identification of the Newton's constant $\kappa_5 = 2\pi/N_c$ dual to pure $\mathcal{N} = 4$ SYM at infinite N_c and infinite 't Hooft coupling λ . For reasons discussed above, the full dual of the action (38) is unknown and we are not aware of a mechanism for deriving this action from a consistent truncation of ten-dimensional type IIB supergravity. Nevertheless, for purposes of comparing the sizes of matter and electromagnetic contributions to the total operator expectation values, it will prove useful to keep the definition of κ_5 in terms of the number of colours N_c of the hypothetical dual deformed $\mathcal{N} = 4$ SYM coupled to dynamical electromagnetism.

To show further evidence that the action (38) is a sensible dual of a strongly coupled MHD plasma, it is useful to elucidate the connection between Eq. (38) and the Einstein-Maxwell theory. To put an uncharged holographic theory in an external magnetic field, one normally adds the Maxwell action F^2 with $F = dA$ to the Einstein-Hilbert bulk action. If one imposes the Dirichlet boundary conditions on the bulk one-form A_a , then A_a sources the R-current J_R^μ at the boundary, $\int d^4x J_R^\mu \delta A_\mu$, and thus the electromagnetic field A_μ is external and non-dynamical. The investigation of the physics of such a setup was initiated in [44] and studied in numerous subsequent works, including recent [27, 28, 36, 45, 46]. Instead, one can work in alternative quantisation and impose Neumann boundary conditions on A_a . Such a choice exchanges the interpretation of the normalisable and the non-normalisable mode in A_a . From the dual field theory point of view, this can be interpreted as the Legendre transform of the boundary coupling, leading to the variation $\int d^4x A_\mu \delta J_R^\mu$. Physically, this means that in alternative quantisation, an external current sources a dynamical (boundary) vector field (see e.g. [47, 48]). The two boundary theories, one with Dirichlet and one with Neumann boundary conditions, are related by a double-trace deformed RG flow.⁸ Since J_R^μ is conserved, one can express it through an anti-symmetric $b_{\mu\nu}$ as $\epsilon^{\mu\nu\rho\sigma} \partial_\nu b_{\rho\sigma}$, which, upon integration by parts, yields a dualised $\int d^4x J^{\mu\nu} \delta b_{\mu\nu}$, where $J^{\mu\nu}$ is the anti-symmetric current from Eq. (11).

⁷ Throughout this paper, we use Greek and Latin letters to denote the boundary and bulk theory indices, respectively.

⁸ See Refs. [49–52] and references therein.

From the point of view of the bulk, as in a lower-dimensional theory [53], the Einstein-Maxwell bulk (quantum) path integral runs over the metric and the Maxwell field A_a . Alternatively, one can write the path integral over the fields strength F_{ab} , but at the expense of ensuring the Bianchi identity $dF = 0$ by introducing a Lagrange multiplier B_{ab} :

$$Z \supset \int \mathcal{D}F_{ab} \mathcal{D}B_{ab} \exp \left\{ i \frac{N_c^2}{8\pi^2} \int d^5x \sqrt{-G} \left(F_{ab} F^{ab} + e_H^{-1} B_{ab} \epsilon^{abcde} \nabla_c F_{de} \right) \right\}. \quad (39)$$

Since the second (Bianchi identity) term vanishes for any classical field solution, it has no influence on the saddle point of the path integral. However, it does generate a non-zero contribution to the boundary action, i.e. $(N_c^2/8\pi^2 e_H) \int d^4x \epsilon^{\mu\nu\rho\sigma} F_{\rho\sigma} B_{\mu\nu}$, which is precisely the source term $\int d^4x J^{\mu\nu} b_{\mu\nu}$ once we identify $B_{\mu\nu} \sim b_{\mu\nu}$ and $J^{\mu\nu} \sim \epsilon^{\mu\nu\rho\sigma} F_{\rho\sigma}$. The precise dictionary between the bulk and boundary quantities will be discussed in Section III B. By varying the action with respect to F_{ab} , one obtains the equation of motion

$$F^{ab} = e_H^{-1} \epsilon^{abcde} \nabla_c B_{de}. \quad (40)$$

Then, the field strength F_{ab} can be integrated out in the saddle point approximation which gives the two-form gauge field Lagrangian term from Eq. (38). Furthermore, in the language of the Einstein-Maxwell theory, by using Eq. (40), one finds the relation between the one-form R-current J_R^μ and the B_{ab} field:

$$\langle J_R^\mu \rangle = -\frac{N_c^2}{2\pi^2} \lim_{u \rightarrow 0} F^{u\mu} = -\frac{N_c^2}{2\pi^2 e_H} \lim_{u \rightarrow 0} \epsilon^{\mu\nu\rho\sigma} \partial_\nu B_{\rho\sigma}, \quad (41)$$

where u is the radial coordinate and $u = 0$ the boundary of the bulk spacetime. Thus, imposing the Dirichlet boundary condition on B_{ab} corresponds to treating J_R^μ as a source, which is the same as performing alternative quantisation discussed above. This is consistent with the interpretation that the dual field theory of (38) contains dynamical photons. Furthermore, as we will see from a detailed holographic renormalisation in Section III B, the boundary counter-terms, which are required to keep the on-shell action finite, will give us precisely the Maxwell theory for A_μ (dual of $b_{\mu\nu}$) on the boundary, including a renormalised electromagnetic coupling e_r , as in QED.⁹ All further details of this holographic setup will be presented in Section III.

III. HOLOGRAPHIC ANALYSIS: EQUATION OF STATE AND TRANSPORT COEFFICIENTS

In this section, we study the relevant details of the simplest holographic theory with Einstein gravity coupled to a two-form bulk field, cf. (38), which can source a two-form current associated with the $U(1)$ generalised global symmetry in the boundary theory. As our goal is to study the phenomenology of MHD waves in a strongly coupled plasma using the dispersion relations of [22],

⁹ We note that the way the Maxwell Lagrangian arises on the boundary is equivalent to the way holographic matter can be coupled to dynamical gravity on a cut-off brane [54]. There too, a holographic counter-term gives rise to the Einstein-Hilbert action at the cut-off brane (the boundary) of a more intricately foliated bulk. As shown by Gubser in [54], such a theory can result in a radiation (CFT)-dominated FRW universe at the boundary with the stress-energy tensor of the $\mathcal{N} = 4$ SYM driving the expansion.

we will use holography only to provide us with the necessary microscopic data: the equation of state and the transport coefficients.

In Section III A, we will begin by discussing details of the magnetic brane solution [44, 55] supported by the bulk action introduced in Section II B. In Section III B, we will consider holographic renormalisation of the theory in question and show how the bulk gives rise to a dual theory coupled to dynamical electromagnetism (as in Section II). In particular, we will derive the expectation values of the stress-energy tensor $\langle T^{\mu\nu} \rangle$ and the two-form $\langle J^{\mu\nu} \rangle$ and show that they satisfy the Ward identities (8) and (9). We will also recover and match all expected renormalisation group properties, such as the beta function of the electromagnetic coupling, from the point of view of the bulk calculation. In Section III C, we will then compute and analyse thermal and magnetic properties of the equation of state of the dual plasma. Finally, in Section III D, we will derive the membrane paradigm formulae for the seven transport coefficients required to describe first-order dissipative MHD [22] and compute them.¹⁰ Further details regarding the horizon formulae for the transport coefficients can be found in Appendix B.

A. Holographic action and the magnetic brane

A holographic action dual to a plasma state with a low-energy limit that can be described by MHD was stated in Eq. (38). Including the boundary Gibbons-Hawking term and the (relevant) holographic counter-term, the full action is

$$S = \frac{N_c^2}{8\pi^2} \left[\int d^5x \sqrt{-G} \left(R + 12 - \frac{1}{3e_H^2} H_{abc} H^{abc} \right) + \int_{\partial M} d^4x \sqrt{-g} \left(2 \text{tr} K - 6 + \frac{1}{e_H^2} \mathcal{H}_{\mu\nu} \mathcal{H}^{\mu\nu} \ln \mathcal{C} \right) \right], \quad (42)$$

where $\text{tr} K$ is the trace of the extrinsic curvature of the boundary (∂M) defined by an outward normal vector n^a . For convenience, we now set $e_H = 1$. The two-form $\mathcal{H}_{\mu\nu}$ is defined as a projection of the three-form field strength in the direction normal the boundary, $\mathcal{H}_{\mu\nu} = n^a H_{a\mu\nu}$. \mathcal{C} is a dimensionless number that needs to be adjusted to fix the renormalisation condition, of which the details will be discussed below. The equations of motion that follow are

$$R_{ab} + 4G_{ab} - \left(H_{acd} H_b{}^{cd} - \frac{2}{9} G_{ab} H_{cde} H^{cde} \right) = 0, \quad (43)$$

$$\frac{1}{\sqrt{-G}} \partial_a \left(\sqrt{-G} H^{abc} \right) = 0. \quad (44)$$

Since the theory (42) is S-dual to the Einstein-Maxwell theory, we can express the magnetised

¹⁰ These horizon formulae are analogous to the expression for shear viscosity in $\mathcal{N} = 4$ theory [56]. For more recent discussions of other transport coefficients that can be computed directly from horizon data, see e.g. [57–63].

black brane solution of [44] by dualising the Maxwell terms and writing

$$\begin{aligned}
ds^2 &= G_{ab}dx^a dx^b = r_h^2 \left(-F(u)dt^2 + \frac{e^{2\mathcal{V}(u)}}{v}(dx^2 + dy^2) + \frac{e^{2\mathcal{W}(u)}}{w}dz^2 \right) + \frac{du^2}{4u^3 F(u)}, \\
H &= \frac{Br_h^2 e^{-2\mathcal{V}+\mathcal{W}}}{2u^{3/2}\sqrt{w}} dt \wedge dz \wedge du.
\end{aligned} \tag{45}$$

The equations of motion (43) for this ansatz reduce to three second-order ordinary differential equations (ODE's) for $\{F, \mathcal{V}, \mathcal{W}\}$ and one additional first-order constraint. The equation of motion derived from the variation of the two-form (44) is automatically satisfied. The equations are equivalent to those derived from the Einstein-Maxwell theory [44] upon identification of the Maxwell bulk two-form F with $F = \mathcal{B} dx \wedge dy$, where $\mathcal{B} = Br_h^2/v$.¹¹

The undetermined functions F , \mathcal{V} and \mathcal{W} can be obtained numerically by using the shooting method. We first expand the background fields near the horizon as

$$\begin{aligned}
F &= f_1^h(1-u) + f_2^h(1-u)^2 + \mathcal{O}(1-u)^3, \\
\mathcal{V} &= v_0^h + v_1^h(1-u) + \mathcal{O}(1-u)^2, \\
\mathcal{W} &= w_0^h + w_1^h(1-u) + \mathcal{O}(1-u)^2,
\end{aligned} \tag{46}$$

where the constants $\{f_i^h, v_i^h, w_i^h\}$ can be written in terms of $\{f_1^h, v_0^h, w_0^h\}$ after solving the equations of motion order-by-order near the horizon. The scaling symmetry of our background ansatz then allows us to rescale dx and dy so that $v_0^h = w_0^h = 0$. Next, we match the numerical solutions generated by shooting from the horizon towards the boundary, where the analytical near-boundary expansions of the metric functions are

$$\begin{aligned}
F &= \frac{1}{u} \left(1 + f_1^b \sqrt{u} + \frac{f_1^b}{4} u + f_4^b u^2 + \mathcal{O}(u^{3/2}) + \left(\frac{\mathcal{B}^2}{3} + \mathcal{O}(\sqrt{u}) \right) u^2 \ln u \right), \\
e^{2\mathcal{V}} &= \frac{1}{u} \left(v + v f_1^b \sqrt{u} + \frac{v(f_1^b)^2}{4} u + v_4^b u^2 + \mathcal{O}(u^{3/2}) - \left(\frac{\mathcal{B}^2}{6} + \mathcal{O}(\sqrt{u}) \right) u^2 \ln u \right), \\
e^{2\mathcal{W}} &= \frac{1}{u} \left(w + w f_1^b \sqrt{u} + \frac{w(f_1^b)^2}{4} u - \frac{2wv_4^b}{v} u^2 + \mathcal{O}(u^{3/2}) - \left(\frac{w\mathcal{B}^2}{3} + \mathcal{O}(\sqrt{u}) \right) u^2 \ln u \right).
\end{aligned} \tag{47}$$

As before, one can solve for the coefficients $\{f_i^b, v_i^b, w_i^b\}$ in terms of $\{f_1^b, f_4^b, v_4^b\}$. Furthermore, f_1^b can be removed by residual diffeomorphism freedom of the metric ansatz [45]. For a given value of $B = v\mathcal{B}/r_h^2$, we can therefore generate a numerical background by shooting from the initial conditions of the functions set by the near-horizon expansion with $\{f_1^h, v_0^h, w_0^h\} = \{\hat{f}, 0, 0\}$. The numerical value of \hat{f} is chosen so that the near-boundary expansion has $f_1^b = 0$. The near-boundary behaviour of this function then determines the properties of the dual field theory. Note that the theory is governed by a one-parameter family of such numerical solutions characterised by the dimensionless ratio $T/\sqrt{\mathcal{B}}$, where $T = f_1^h r_h/2\pi$ is the Hawking temperature (see Eq. (83)). In practice, this ratio can be tuned by changing the parameter B of the background ansatz. The

¹¹ The metric ansatz is chosen to have the form used in [45]. It can be obtained from the ansatz $ds^2 = -U(r)dt^2 + e^{2V(r)}(dx^2 + dy^2) + e^{2W(r)}dz^2 + dr^2/U(r)$ used in [44] by performing a coordinate transformation $r = r_h/\sqrt{u}$ and shifting V and W by constant $-\ln v$ and $-\ln w$, respectively, which are chosen so that the near-boundary expansion has the form $ds^2 = (1/u)\eta_{\mu\nu}dx^\mu dx^\nu + du^2/(4u^2)$.

numerical solver encounters stiffness problems when $B \approx \sqrt{3}$, i.e. where the temperature is close to zero. All of our numerical results will therefore stop near $T/\sqrt{B} = 0$. In this work, we do not attempt an independent analysis of the theory at $T = 0$.

B. Holographic renormalisation and the bulk/boundary dictionary

The next step in analysing the dual of (42) is a systematic holographic renormalisation. In this section, we derive the one-point functions of the stress-energy tensor $\langle T_{\mu\nu} \rangle$ and the two-form current $\langle J_{\mu\nu} \rangle$, and show that they satisfy the Ward identities of magnetohydrodynamics (8) and (9) [22], which in terms of operator expectation values take the form

$$\nabla_\nu \langle T^{\mu\nu} \rangle = \tilde{H}^\mu{}_{\lambda\sigma} \langle J^{\lambda\sigma} \rangle, \quad \nabla_\mu \langle J^{\mu\nu} \rangle = 0, \quad (48)$$

where $\tilde{H} = db$ is the field strength of the background gauge field b in field theory. The precise definition of these quantities will become clear below. Since we are only interested in the expansion of MHD to first order in the gradient expansion around a flat (boundary) background, it will be sufficient to only work with terms that contain no more than two derivatives along the boundary directions. The procedure for obtaining holographic renormalisation will closely follow Refs. [64, 65].¹²

We begin by writing the bulk metric in the Fefferman-Graham coordinates [64]

$$ds_{\text{FG}}^2 = G_{ab} dx^a dx^b = \frac{d\rho^2}{4\rho^2} + \gamma_{\mu\nu}(\rho, x) dx^\mu dx^\nu = \frac{d\rho^2}{4\rho^2} + \frac{1}{\rho} g_{\mu\nu}(\rho, x) dx^\mu dx^\nu, \quad (49)$$

so that near the boundary, $\rho \approx 0$, the metric $g_{\mu\nu}$ can be expanded as

$$g_{\mu\nu}(\rho, x) = g_{\mu\nu}^{(0)}(x) + \rho g_{\mu\nu}^{(1)}(x) + \rho^2 \left(g_{\mu\nu}^{(2)}(x) + \tilde{h}_{\mu\nu}(x) \ln \rho \right) + \mathcal{O}(\rho^3). \quad (50)$$

Note that Greek (boundary) indices in a tensor $A^{\mu\nu}$ are raised with the metric $g_{(0)}^{\mu\nu}$, which satisfies $g_{\mu\nu}^{(0)} g_{(0)}^{\mu\nu} = 4$. There are two types of covariant derivative that we will use: $\nabla_\mu^{(g)}$ and ∇_μ . Firstly, $\nabla_\mu^{(g)}$ and $\nabla_{(g)}^\mu \equiv g^{\mu\nu} \nabla_\nu^{(g)}$ are defined with respect to the metric $g_{\mu\nu}(\rho, x)$, while ∇_μ and $\nabla^\mu \equiv g_{(0)}^{\mu\nu} \nabla_\nu$ are defined through the metric $g_{\mu\nu}^{(0)}(x)$. The Ricci tensors of $g_{\mu\nu}$ and $g_{\mu\nu}^{(0)}$ are denoted by $R_{\mu\nu}^{(g)}$ and $R_{\mu\nu}^{(0)}$, respectively.

The components of bulk two-form gauge field B_{ab} in the boundary field theory directions can similarly be expanded near the boundary as

$$B_{\mu\nu}(\rho, x) = B_{\mu\nu}^{(0)}(x) + B_{\mu\nu}^{(1)}(x) \ln \rho + \mathcal{O}(\rho). \quad (51)$$

In the boundary directions, the three-form field strength is defined as $H_{\mu\nu\sigma} = \partial_\mu B_{\nu\sigma} + \partial_\nu B_{\sigma\mu} + \partial_\sigma B_{\mu\nu}$, with the near-boundary expansion $H_{\mu\nu\sigma}(\rho, x) = H_{\mu\nu\sigma}^{(0)}(x) + H_{\mu\nu\sigma}^{(1)}(x) \ln \rho + \mathcal{O}(\rho)$. Each $H^{(n)}$ is defined in terms of $B^{(n)}$, i.e. in the same way at each order. Note that both quantities $B_{\mu\nu}^{(0)}$ and $B_{\mu\nu}^{(1)}$ are related to the two-form gauge field source of the boundary theory, $\int d^4x \sqrt{-g} J^{\mu\nu} \delta b_{\mu\nu}$.

¹² This part of the calculation was performed by using the Mathematica package xAct [66].

The variation of the bulk on-shell contribution from the H^2 term, evaluated at the boundary cutoff $\rho = \rho_\Lambda$, is

$$\delta S_{on-shell} = -\frac{N_c^2}{4\pi^2} \int d^4x \sqrt{-g} \mathcal{H}^{\mu\nu} \left(\delta B_{\mu\nu}^{(0)} + \delta B_{\mu\nu}^{(1)} \ln \mathcal{C}^2 \rho_\Lambda \right). \quad (52)$$

The expectation value of the operator sourced by $B_{\mu\nu}^{(0)}$ and $B_{\mu\nu}^{(1)}$ depends on N_c^2 . However, since, by definition, $J^{\mu\nu} = \frac{1}{2} \epsilon^{\mu\nu\lambda\sigma} F_{\lambda\sigma}$, of which the expectation value contains no colour trace, we need to identify the combination of $B_{\mu\nu}^{(0)}$ and $B_{\mu\nu}^{(1)}$, and the field theory source $b_{\mu\nu}$ as

$$B_{\mu\nu}^{(0)} + B_{\mu\nu}^{(1)} \ln \mathcal{C}^2 \rho_\Lambda = \frac{4\pi^2}{N_c^2} b_{\mu\nu}. \quad (53)$$

The expectation value of $J^{\mu\nu}$ can then be obtained by taking a variational derivative of the on-shell action with respect to the source $b_{\mu\nu}$.

The Ward identities (48) can be obtained by solving the equations of motion (43) and (44) [65]. In Fefferman-Graham coordinates (49), these equations (together with the trace of (43)) become

$$\frac{1}{2} \text{tr} [g^{-1} g''] - \frac{1}{4} \text{tr} [g^{-1} g' g^{-1} g'] + \frac{1}{3} \rho^2 \text{tr} [g^{-1} B' g^{-1} B'] - \frac{1}{18} \rho \text{tr} [g^{-1} H^2] = 0, \quad (54)$$

$$\frac{1}{2} \left(\nabla_\mu^{(g)} \text{tr} g' - \nabla_{(g)}^\nu g'_{\mu\nu} \right) - \rho^2 H_{\mu\alpha\beta} (g^{-1} B' g^{-1})^{\alpha\beta} = 0, \quad (55)$$

$$\rho \left(2g''_{\mu\nu} - 2(g' g^{-1} g')_{\mu\nu} + g'_{\mu\nu} \text{tr} [g^{-1} g'] \right) + R_{\mu\nu}^{(g)} - 2g'_{\mu\nu} - g_{\mu\nu} \text{tr} [g^{-1} g'] + 8\rho^3 \left((B' g^{-1} B')_{\mu\nu} - \frac{1}{3} g_{\mu\nu} \text{tr} [g^{-1} B' g^{-1} B'] \right) + \rho^2 \left(H_{\mu\nu}^2 - \frac{2}{9} g_{\mu\nu} \text{tr} [g^{-1} H^2] \right) = 0, \quad (56)$$

$$\frac{d}{d\rho} \left(2\rho (g^{-1} B' g^{-1})^{\mu\nu} \right) + \frac{1}{2} \nabla_{(g)}^\lambda \left(g^{\mu\alpha} g^{\nu\beta} H_{\lambda\alpha\beta} \right) = 0, \quad (57)$$

$$\nabla_\nu (g^{-1} B' g^{-1})^{\mu\nu} = 0, \quad (58)$$

where g^{-1} denotes the matrix inverse of g (in components, this is $g^{\mu\nu}$) and where

$$\text{tr} [g^{-1} B' g^{-1} B'] = -B'_{\mu_1\mu_2} B'_{\nu_1\nu_2} g^{\mu_1\nu_1} g^{\mu_2\nu_2}, \quad H_{\mu\nu}^2 = H_{\mu\lambda_1\lambda_2} H_{\nu\sigma_1\sigma_2} g^{\lambda_1\sigma_1} g^{\lambda_2\sigma_2}. \quad (59)$$

Expanding equations (54)–(58) around small ρ , we find that

$$g_{\mu\nu}^{(1)} = \frac{1}{2} \left(R_{\mu\nu}^{(0)} - \frac{1}{6} g_{\mu\nu}^{(0)} R^{(0)} \right), \quad (g^{(1)})^\mu{}_\mu = \frac{1}{6} R. \quad (60)$$

Since $g_{\mu\nu}^{(1)}$ is proportional to second derivatives of the boundary metric, and we are only keeping track of terms up to second orders in boundary derivatives, we can ignore terms with $g_{\mu\nu}^{(1)}$. The remaining equations of motion can thus be written as

$$(g^{(2)})^\mu{}_\mu - \frac{1}{3} B_{\mu\nu}^{(1)} B^{(1)\mu\nu} = 0, \quad \tilde{h}^\mu{}_\mu = 0, \quad \nabla_\nu B^{(1)\mu\nu} = 0, \quad (61)$$

$$-H_{\mu\nu\lambda}^{(0)} B^{(1)\nu\lambda} + \nabla_{(0)}^\nu \left(g_{\mu\nu}^{(0)} (g^{(2)})^\lambda{}_\lambda - g_{\mu\nu}^{(2)} - \frac{1}{2} \tilde{h}_{\mu\nu} \right) = 0, \quad (62)$$

$$\tilde{h}_{\mu\nu} + \frac{1}{2} \left(4B_{\mu\lambda}^{(1)} (B^{(1)})^\lambda{}_\nu - g_{\mu\nu}^{(0)} B_{\lambda\sigma}^{(1)} B^{(1)\lambda\sigma} \right) = 0. \quad (63)$$

The expectation values of the stress-energy tensor and the two-form current follow from the generating functional (37):

$$\langle T^{\mu\nu} \rangle = -\frac{2i}{\sqrt{-g^{(0)}}} \frac{\delta \ln W}{\delta g_{\mu\nu}^{(0)}}, \quad \langle J^{\mu\nu} \rangle = -\frac{i}{\sqrt{-g^{(0)}}} \frac{\delta \ln W}{\delta b_{\mu\nu}}. \quad (64)$$

In holography, W is computed from the (on-shell) action (42), giving us¹³

$$\langle T_{\mu\nu} \rangle = -\frac{N_c^2}{4\pi^2} \lim_{\epsilon \rightarrow 0} \frac{r^2}{\epsilon} \left(K_{\mu\nu} - \gamma_{\mu\nu} K - 3\gamma_{\mu\nu} + \frac{1}{2} R[\gamma]_{\mu\nu} - \frac{1}{4} \gamma_{\mu\nu} R[\gamma] - \left(\mathcal{H}_{\mu\lambda} \mathcal{H}_\nu^\lambda - \frac{1}{4} \gamma_{\mu\nu} \mathcal{H}_{\alpha\beta} \mathcal{H}^{\alpha\beta} \right) \ln(\mathcal{C}\rho) \right) \Big|_{\rho=\epsilon}, \quad (65)$$

$$\langle J_{\mu\nu} \rangle = -\lim_{\epsilon \rightarrow 0} \mathcal{H}_{\mu\nu} \Big|_{\rho=\epsilon}. \quad (66)$$

Note that the expectation value of $T^{\mu\nu}$ scales as N_c^2 , the expectation value of $J^{\mu\nu}$ is of order $\mathcal{O}(1)$.

By using Eq. (61) and the fact that $\mathcal{H}_{\mu\nu} = n^\rho H_{\rho\mu\nu} = -2B_{\mu\nu}^{(1)} + \mathcal{O}(\rho)$, we find that the boundary two-form current is conserved:

$$\nabla_{(0)}^\mu \langle J_{\mu\nu} \rangle = 2\nabla^\mu B_{\mu\nu}^{(1)} = 0. \quad (67)$$

Using the definition (11), which gives $\langle J_{\mu\nu} \rangle = \frac{1}{2} \epsilon_{\mu\nu\rho\sigma} \langle F^{\rho\sigma} \rangle$ and connects Eq. (67) with the Bianchi identity, we find that $\star B^{(1)}$ sets the expectation value of the Maxwell field strength $\langle F \rangle$. Furthermore, the (regularised) stress-energy tensor (65) becomes

$$\langle T_{\mu\nu} \rangle = \lim_{\epsilon \rightarrow 1/\Lambda^2} \frac{N_c^2}{2\pi^2} \left(g_{\mu\nu}^{(2)} - g_{\mu\nu}^{(0)} (g^{(2)})^\lambda_\lambda + \frac{1}{2} \tilde{h}_{\mu\nu} + \tilde{h}_{\mu\nu} \ln(\mathcal{C}^2 \rho) + \mathcal{O}(\rho, \partial^2) \right) \Big|_{\rho=\epsilon}, \quad (68)$$

where Λ is the UV cutoff of the theory. As discussed in Section II, the choice of the dimensionful constant \mathcal{C} must now be made in order to fix the renormalisation condition, which will render the renormalised expectation value $\langle T_{\mu\nu} \rangle$ physical.

To see how the constant \mathcal{C} in Eq. (68) is related to our discussion in Section II, we write the last term by introducing a mass scale M :

$$\frac{N_c^2}{\pi^2} \tilde{h}_{\mu\nu} \ln(\Lambda/\mathcal{C}) = \frac{N_c^2}{\pi^2} \tilde{h}_{\mu\nu} \ln(\Lambda/M) + \tilde{h}_{\mu\nu} \left(\frac{2}{e_r^2} - \frac{N_c^2}{\pi^2} \ln(\Lambda/M) \right). \quad (69)$$

What can be seen from Eq. (69) is that this splitting precisely reproduces the way the logarithmic divergence enters into the stress-energy tensor from two different pieces of the Lagrangian: the matter content (with its coupling to the photons) and the electromagnetic (Maxwell) part:

$$\langle T_{\mu\nu} \rangle = \langle T_{\mu\nu}^{matter} \rangle + \langle T_{\mu\nu}^{EM} \rangle, \quad (70)$$

with the two terms being

$$\langle T_{\mu\nu}^{matter} \rangle = \frac{N_c^2}{2\pi^2} \left(g_{\mu\nu}^{(2)} - g_{\mu\nu}^{(0)} (g^{(2)})^\lambda_\lambda + \frac{1}{2} \tilde{h}_{\mu\nu} \right) - \frac{N_c^2}{\pi^2} \tilde{h}_{\mu\nu} \ln(\Lambda/M), \quad (71)$$

$$\langle T_{\mu\nu}^{EM} \rangle = -\left(\frac{2}{e_r^2} - \frac{N_c^2}{\pi^2} \ln(\Lambda/M) \right) \tilde{h}_{\mu\nu}. \quad (72)$$

¹³ Note that in order to raise indices of the boundary theory expectation values, one needs to use the induced metric $\gamma_{\mu\nu}$.

Finally, we note that the electromagnetic $\langle T_{\mu\nu}^{EM} \rangle$ would follow precisely from the Maxwell boundary action

$$S_{EM} = -\frac{1}{4e(\Lambda/M)^2} \int d^4x \sqrt{-g} F_{\mu\nu} F^{\mu\nu}, \quad (73)$$

upon using Eq. (63) and the fact that the bulk $\star B^{(1)}$ determines $\langle F_{\mu\nu} \rangle$:

$$\begin{aligned} \langle T_{\mu\nu}^{EM} \rangle &= \frac{1}{e(\Lambda/M)^2} \left(\langle F_{\mu\alpha} F_{\nu}{}^{\alpha} \rangle - \frac{1}{4} \eta_{\mu\nu} \langle F_{\alpha\beta} F^{\alpha\beta} \rangle \right) \\ &= \frac{1}{e(\Lambda/M)^2} \left(\langle F_{\mu\alpha} \rangle \langle F_{\nu}{}^{\alpha} \rangle - \frac{1}{4} \eta_{\mu\nu} \langle F_{\alpha\beta} \rangle \langle F^{\alpha\beta} \rangle \right), \end{aligned} \quad (74)$$

where the last equality follows from the fact that quantum fluctuations of the photon field are suppressed in the boundary QFT. Our holographic calculation thus fully reproduces Eq. (33), which followed from the field theory discussion in Section II B. Furthermore, the running electromagnetic coupling constant matches the one found from field theory (cf. Eq. (36)) [36]. Hence, our holographic setup appears to contain the $U(1)$ -gauged matter content of the $\mathcal{N} = 4$ SYM theory. In terms of bulk quantities, the renormalised stress-energy tensor and the two-form current are

$$\langle T_{\mu\nu} \rangle = \frac{N_c^2}{2\pi^2} \left(g_{\mu\nu}^{(2)} - g_{\mu\nu}^{(0)} (g^{(2)})^\lambda{}_\lambda + \frac{1}{2} \tilde{h}_{\mu\nu} \right) - \frac{2}{e_r^2} \tilde{h}_{\mu\nu}, \quad (75)$$

$$\langle J_{\mu\nu} \rangle = 2B_{\mu\nu}^{(1)}, \quad (76)$$

where, as in Section II, e_r is the renormalised coupling which needs to be set by experimental input—the renormalisation condition. In practice, this constant is fixed by choosing the value of \mathcal{C} in (65). For the same reasons as in QFT, there is therefore an inherent ambiguity in holographic results, which has to be fixed by external physically-motivated input.

We conclude this section by noting that the relation (62) and a relation between \tilde{H} , $H^{(0)}$ and $H^{(1)}$ implies that the Ward identity for the stress-energy tensor satisfies Eq. (8), or in terms of our holographic notation, $\nabla_\nu \langle T^{\mu\nu} \rangle = \tilde{H}^\mu{}_{\lambda\sigma} \langle J^{\lambda\sigma} \rangle$, as in Eq. (48).

C. Equation of state

To find the equation of state of our theory, we can use the renormalised stress-energy tensor (75) and the two-form current (76) computed in the previous section. Expressed in terms of the near-boundary expansions (47), which can be read off from the numerical background, we find

$$\langle T^{tt} \rangle = \frac{N_c^2}{2\pi^2} \left[-\frac{3}{4} f_4^b r_h^4 + \frac{\mathcal{B}^2}{8\pi\bar{\alpha}} \right], \quad (77)$$

$$\langle T^{xx} \rangle = \langle T^{yy} \rangle = \frac{N_c^2}{2\pi^2} \left[\left(-\frac{1}{4} f_4^b + \frac{v_4^b}{v} \right) r_h^4 - \frac{\mathcal{B}^2}{4} + \frac{\mathcal{B}^2}{8\pi\bar{\alpha}} \right], \quad (78)$$

$$\langle T^{zz} \rangle = \frac{N_c^2}{2\pi^2} \left[\left(-\frac{1}{4} f_4^b - 2\frac{v_4^b}{v} \right) r_h^4 - \frac{\mathcal{B}^2}{8\pi\bar{\alpha}} \right], \quad (79)$$

where we have used the (renormalised) fine-structure constant $\alpha = e_r^2/4\pi$ of the electromagnetic coupling in the plasma, which, as e_r , is fixed by the choice of \mathcal{C} in (65), and rescaled it by $N_c^2/2\pi^2$ (or $|\beta(1/e^2)|$) as

$$\bar{\alpha} = \frac{N_c^2}{2\pi^2}\alpha. \quad (80)$$

The coupling $\bar{\alpha}$ has to be fixed by experimental observations as in any other quantum field theory, which is not easy in an unrealistic toy model.

In studying strongly coupled MHD, it is phenomenologically relevant to not only consider the matter and light-matter interactions, but to also include large electromagnetic self-interactions encoded in the Maxwell action. However, since we are working with a holographic large- N_c matter sector and a single photon, it is unnatural to expect a Maxwell term of the same order. The choice that we make here is to set the rescaled constant $\bar{\alpha}$ to the physically motivated $\bar{\alpha} = 1/137$. There are several ways to think about this choice: one is imagining that our plasma contains magnetic properties, which have non-trivial scalings with N_c , while another interpretation may assume that the bulk studied here could remain a valid dual of a theory with a reasonably small N_c . Of course, by considering only a classical bulk theory, we are restricting the strict validity of any computed observable to the limit of $N_c \rightarrow \infty$. As soon as one moves towards finite N_c , it becomes crucial to estimate the size of subleading $1/N_c^2$ corrections (topological expansion in the string coupling g_s)—an endeavour in holography (and string theory) which to date has been largely neglected and will continue being neglected in this work.¹⁴ A less problematic limit is that of the infinite 't Hooft coupling, which is also implied by the choice of our action.¹⁵ Perhaps the best interpretation is one of an “agnostic choice” led by our having to fix a free parameter to some value. We will return to a more careful investigation of the dependence of our results on this choice in Section IV C.

The expectation values of the stress-energy tensor expressed in (77)–(79) are related to the MHD stress-energy tensor in Eq. (12) by

$$\langle T^{tt} \rangle = \varepsilon, \quad \langle T^{xx} \rangle = p, \quad \langle T^{zz} \rangle = p - \mu\rho. \quad (81)$$

We note that, as required in a conformal field theory with a trace anomaly induced by electromagnetic interactions, the trace of stress-energy tensor is non-zero. The holographic two-form current,

$$\langle J^{tz} \rangle = \mathcal{B} = \frac{Br_h^2}{v}, \quad (82)$$

is related to the equilibrium magnetic flux line density appearing in the MHD equation (13) as $\langle J^{tz} \rangle = \rho$. Temperature and entropy can be expressed in terms of the background geometry as

$$T = \frac{1}{2\pi} f_1^h r_h, \quad s = \frac{N_c^2}{2\pi^2} \left(\frac{\pi r_h^3}{v\sqrt{w}} \right), \quad (83)$$

¹⁴ For some discussions of $1/N_c^2$ corrections to the thermodynamic free energy (the equilibrium partition function) and hydrodynamic long-time tails, see [67–69].

¹⁵ For recent discussions of coupling-dependent holography, see [70–74] and references therein.

and are therefore independent of the renormalised electromagnetic charge. The chemical potential, which corresponds to the density of magnetic flux lines, can be computed by using the thermodynamic identity $\varepsilon + p = sT + \mu\rho$ (cf. (20)):

$$\mu = \frac{\langle T^{xx} \rangle - \langle T^{zz} \rangle}{\langle J^{tz} \rangle} = \frac{N_c^2}{2\pi^2} \left(\frac{3v_4^b}{B} - \frac{B}{4v} + \frac{B}{4\pi v\bar{\alpha}} \right) r_h^2. \quad (84)$$

Note that with our choice of the bulk theory scalings, $\rho \sim \mathcal{O}(1)$ and $\mu \sim \mathcal{O}(N_c^2)$. Furthermore, while $T \sim \mathcal{O}(1)$, p , ε and s all scale as $\mathcal{O}(N_c^2)$.

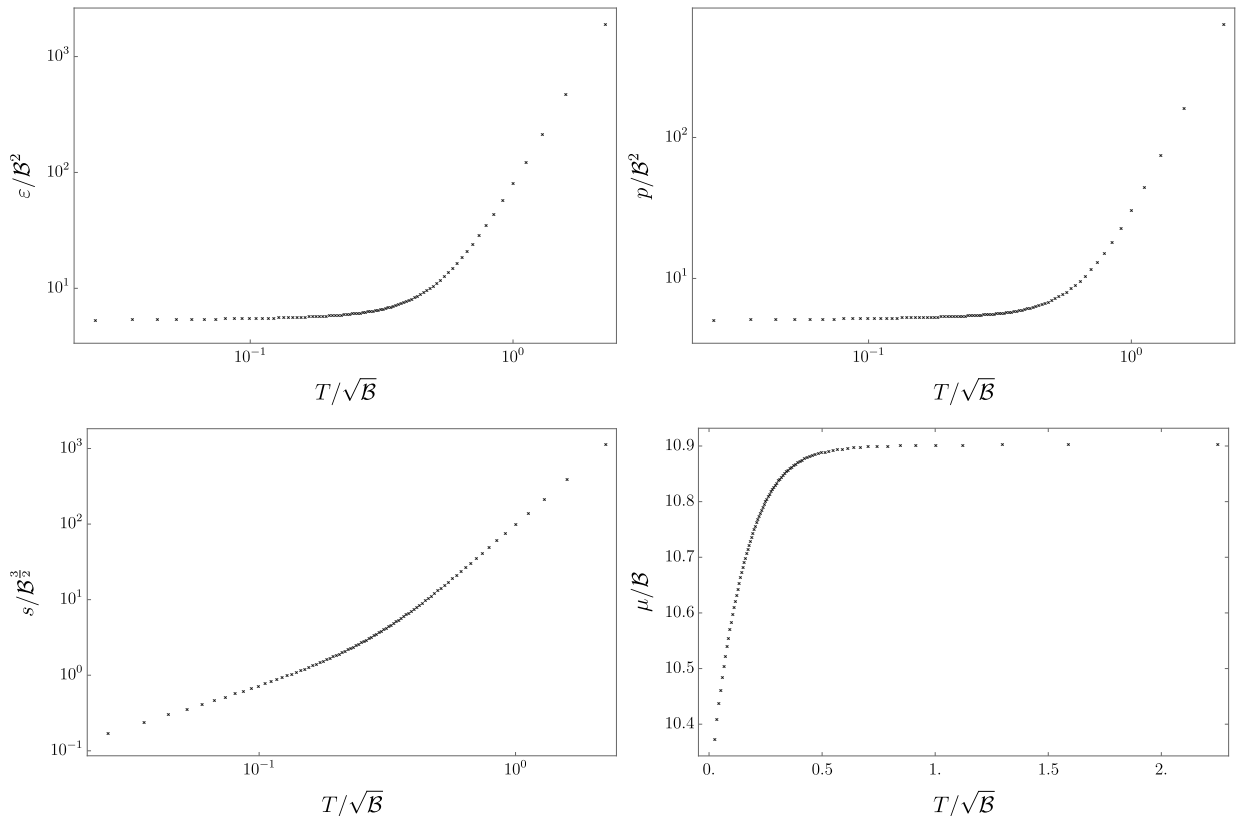


FIG. 1. Dimensionless energy density ε/B^2 (top-left), pressure p/B^2 (top-right), entropy density $s/B^{3/2}$ (bottom-left) and chemical potential μ/B (bottom-right), in units of $N_c^2/(2\pi^2)$, plotted as a function of the dimensionless parameter T/\sqrt{B} . The first three plots use logarithmic scales on both axes.

Using the above relations, we can perform two consistency checks on our holographic setup and numerical calculations of the background. First, the value of the pressure computed from the stress-energy tensor component $\langle T^{xx} \rangle = p$ can be compared with the value of the Euclidean on-shell action, $p = -i(\beta V_3)^{-1} S_{on-shell}$, where $\beta = 1/T$ and V_3 is the spatial volume of the theory. Secondly, we can compute $\varepsilon + p - \mu\rho$ from the stress-energy tensor evaluated near the boundary and by using the thermodynamic relation (20), check whether its values agrees with sT computed purely from horizon quantities. Both calculations show consistency of our setup in that we find $\langle T^{xx} \rangle = -i(\beta V_3)^{-1} S_{on-shell}$ and $\langle T^{tt} \rangle + \langle T^{zz} \rangle = sT$, within numerical precision.

We can now plot various thermodynamic quantities in a dimensionless manner by dividing them by appropriate powers of B . The natural dimensionless parameter with respect to which

we present our numerical results is $T/\sqrt{\mathcal{B}}$. The results for the energy density, pressure, entropy density and chemical potential are shown in Figure 1. The theory has two distinct regimes: the low- and the high-temperature regimes, or alternatively, the strong and weak magnetic field regimes, respectively. The high-temperature regime $T/\sqrt{\mathcal{B}} \gg 1$ is one to which MHD has been historically applied and to which the formulation of MHD, which assumes a weak-field separation between fluid and charge degrees of freedom can be applied. The claim presented in the Ref. [22] is that within the dual formulation, however, MHD applies for all values of $T/\sqrt{\mathcal{B}}$ provided that the state remains in the hydrodynamic regime. The profiles of the thermodynamic functions in Figure 1 show a smooth crossover between the two regimes, which occurs around

$$T/\sqrt{\mathcal{B}} \approx 0.5 - 0.7. \quad (85)$$

By using numerical fits, the equation of state in the two limits behaves as expected on dimensional grounds [22]. We present our numerical results in Table I.

	weak field ($T/\sqrt{\mathcal{B}} \gg 1$)	strong field ($T/\sqrt{\mathcal{B}} \ll 1$)
ε	$\frac{N_c^2}{2\pi^2} (74.1 \times T^4)$	$\frac{N_c^2}{2\pi^2} (5.62 \times \mathcal{B}^2)$
p	$\frac{N_c^2}{2\pi^2} (25.3 \times T^4)$	$\frac{N_c^2}{2\pi^2} (5.32 \times \mathcal{B}^2)$
s	$\frac{N_c^2}{2\pi^2} (99.4 \times T^3)$	$\frac{N_c^2}{2\pi^2} (7.41 \times \mathcal{B} T)$
μ	$\frac{N_c^2}{2\pi^2} (10.9 \times \mathcal{B})$	$\frac{N_c^2}{2\pi^2} (2.88 \times \mathcal{B})$

TABLE I. Approximate asymptotic behaviour of the equation of state in weak- and strong-field limits for $\bar{\alpha} = 1/137$.

In the limit of $\mathcal{B} \rightarrow 0$, the weak-field result approximately limits to the equation of state of a strongly coupled, thermal $\mathcal{N} = 4$ plasma, dual to a five dimensional AdS-Schwarzschild black brane with $p_{\mathcal{N}=4} = \frac{1}{8} N_c^2 \pi^2 T^4$; i.e. $\lim_{\mathcal{B} \rightarrow 0} p_{weak} \approx 1.28 \times N_c^2 T^4$ and $p_{\mathcal{N}=4} \approx 1.23 \times N_c^2 T^4$. We also note that the value of the pressure at low temperature strongly depends on the renormalised (re-scaled) fine structure constant $\bar{\alpha}$, which we set to $\bar{\alpha} = 1/137$.

D. Transport coefficients

Next, we compute the seven transport coefficients, η_{\perp} , η_{\parallel} , r_{\perp} , r_{\parallel} , ζ_{\perp} , ζ_{\parallel} and ζ_{\times} , by using the Kubo formulae derived in [22, 25] and reviewed in Appendix A. The procedure only requires us to turn on time-dependent fluctuations of the background fields without any spatial dependence, $G_{ab} \rightarrow G_{ab} + \delta G_{ab}(t)$ and $B_{ab} \rightarrow B_{ab} + \delta B_{ab}(t)$. The perturbations asymptote to the boundary sources $\delta g_{\mu\nu}^{(0)}$ and $\delta b_{\mu\nu}^{(0)}$ of the dual stress-energy tensor and the two-form current. In the absence of spatial dependence, the fluctuations decouple into five separate channels, from which the seven transport coefficients are computed, with each channel containing one independent dynamical second-order equation. The sets of decoupled fluctuations responsible for their respective transport

coefficients are

$$\begin{aligned}
\eta_{\perp} &: \delta G_{xy}, \\
\eta_{\parallel} &: \delta G_{xz}, \delta B_{tx}, \delta B_{xu}, \\
\zeta_{\perp}, \zeta_{\parallel}, \zeta_{\times} &: \delta G_{tt}, \delta G_{xx}, \delta G_{yy}, \delta G_{zz}, \delta B_{tz}, \delta G_{tu}, \delta B_{zu}, \delta G_{uu}, \\
r_{\perp} &: \delta B_{xz}, \delta G_{tx}, \delta G_{xu}, \\
r_{\parallel} &: \delta B_{xy},
\end{aligned} \tag{86}$$

with only one of the three bulk viscosities being independent. Each one of the transport coefficients can then be related to a membrane paradigm formula and computed entirely in terms of the horizon quantities. We summarise these relations here and discuss their derivation below:

$$\begin{aligned}
\eta_{\perp} &= \frac{N_c^2}{2\pi^2} \left(\frac{r_h^3}{4v\sqrt{w}} \right) = \frac{1}{4\pi} s, \\
\eta_{\parallel} &= \frac{N_c^2}{2\pi^2} \left(\frac{r_h^3}{4w^{3/2}} \right) = \frac{1}{4\pi} \frac{v}{w} s, \\
r_{\perp} &= \frac{2\pi^2}{N_c^2} \left(\frac{\sqrt{w}}{r_h} \right) \left(\frac{\mathfrak{b}_{xz}^{(-)}(1)}{\mathfrak{b}_{xz}^{(-)}(0)} \right)^2, \\
r_{\parallel} &= \frac{2\pi^2}{N_c^2} \left(\frac{v}{r_h\sqrt{w}} \right), \\
\zeta_{\perp} = \frac{1}{4}\zeta_{\parallel} = -\frac{1}{2}\zeta_{\times} &= \frac{N_c^2}{2\pi^2} \left(\frac{r_h^3}{12v\sqrt{w}} \left(\frac{6+B^2}{6-B^2} \right)^2 \left[\frac{\mathfrak{Z}^{(-)}(1)}{\mathfrak{Z}^{(-)}(0)} \right]^2 \right),
\end{aligned} \tag{87}$$

where $\mathfrak{b}^{(-)}$ and $\mathfrak{Z}^{(-)}$ are the time-independent solutions of the fluctuations δB_{xz} and $Z_s = \delta G_x^x + \delta G_y^y - (2\mathcal{V}'/\mathcal{W}')\delta G_z^z$, respectively. The arguments denote that the functions are evaluated either at the horizon, $u = 1$, or the boundary, $u = 0$. Note that the value at the boundary is set by the Dirichlet boundary conditions.

What we see is that the ratio of the transverse shear viscosity (w.r.t. the background magnetic field) to entropy density is universal, resulting in $\eta_{\perp}/s = 1/4\pi$. Furthermore, the expressions for η_{\parallel} and r_{\parallel} only depend on the background quantities v and w , while ζ_{\perp} , ζ_{\parallel} and r_{\perp} also depend on the fluctuations of the fields.¹⁶

In order to derive the horizon formulae, we use the Wronskian method (see e.g. [61]). Here, we will only explicitly show the derivation of the transverse resistivity r_{\perp} . The other formulae from Eq. (87) are derived in Appendix B. First, we combine the equations of motion for the relevant fluctuations, δB_{xz} , δG_{tx} , and δG_{xu} , into a single second-order differential equation by eliminating the metric fluctuations,

$$\delta B_{xz}'' + \left(\frac{3}{2u} + \frac{F'}{F} - \mathcal{W}' \right) \delta B_{xz}' + \left(\frac{\omega^2}{4r_h^2 u^3 F^2} - \frac{B^2 e^{-4V}}{u^3 F} \right) \delta B_{xz} = 0. \tag{88}$$

Since we are only computing first-order transport coefficients, it is sufficient to solve Eq. (88) to linear order in ω . To find the solution, we assume that there exists a time-independent solution $\mathfrak{b}_{xz}^{(-)}(u)$, which asymptotes to a constant both at the boundary and the horizon. At the

¹⁶ For a holographic derivation of bulk viscosity in neutral relativistic hydrodynamics, see [57].

boundary, this asymptotic value is related to the source of the two-form background gauge field, i.e. $\mathfrak{b}_{xz}^{(-)}(u \rightarrow 0) = \delta B_{xz}^{(0)}$. The time-dependent information is contained in the second solution, linearly-independent from $\mathfrak{b}_{xz}^{(-)}$. We refer to this solution as $\mathfrak{b}_{xz}^{(+)}$. It can be expressed as an integral over the Wronskian W_R of (88):

$$\mathfrak{b}_{xz}^{(+)}(u) = \mathfrak{b}_{xz}^{(-)}(u) \int_u^1 du' \frac{W_R(u')}{\left(\mathfrak{b}_{xz}^{(-)}(u')\right)^2}, \quad (89)$$

where

$$W_R(u) = \exp \left[- \int_u^1 du' \left(\frac{3}{2u'} + \frac{F'(u')}{F(u')} - \mathcal{W}'(u') \right) \right] = \frac{1}{u^{3/2} F e^{-\mathcal{W}}}. \quad (90)$$

The near-boundary and the near-horizon expansions of $\mathfrak{b}_{xz}^{(+)}$ are

$$\mathfrak{b}_{xz}^{(+)} = \begin{cases} \sqrt{w} \left[\mathfrak{b}_{xz}^{(-)}(0) \right]^{-1} \ln u + \mathcal{O}(\sqrt{u}), & \text{for } u \approx 0, \\ -r_h \left[2\pi T \mathfrak{b}_{xz}^{(-)}(1) \right]^{-1} \ln(1-u) + \mathcal{O}(1-u), & \text{for } u \approx 1. \end{cases} \quad (91)$$

Finally, $\delta B_{xz}(\omega, u)$ is then the following linear combination of the two solutions:

$$\delta B_{xz}(\omega, u) = \mathfrak{b}_{xz}^{(-)}(u) + \alpha(\omega) \mathfrak{b}_{xz}^{(+)}(u) + \mathcal{O}(\omega^2). \quad (92)$$

The coefficient $\alpha(\omega)$ can be determined by imposing regular ingoing boundary conditions at the horizon, which corresponds to computing a retarded dual correlator [75, 76]:

$$\delta B_{xz}(u) = (1-u)^{-\frac{i\omega}{4\pi T}} \tilde{B}_{xz}. \quad (93)$$

The function $\tilde{B}_{xz}(u)$ is regular at the horizon. This choice of the boundary condition implies that near the horizon, δB_{xz} behaves as

$$\delta B_{xz}(u) = \mathfrak{b}_{xz}^{(-)}(u) + \alpha(\omega) \mathfrak{b}_{xz}^{(+)}(u) + \dots = \mathfrak{b}_{xz}^{(-)}(1) \left(1 - \frac{i\omega}{4\pi T} \ln(1-u) \right) + \dots \quad (94)$$

Comparing Eq. (94) with the asymptotic behaviour of $\mathfrak{b}_{xz}^{(+)}$ in (91), we find $\alpha = (i\omega/2r_h) \left[\mathfrak{b}_{xz}^{(-)}(1) \right]^2$. Thus, the near-boundary expression for δB_{xz} becomes

$$\delta B_{xz}(u) = \mathfrak{b}_{xz}^{(-)}(0) \left(1 + \frac{i\omega}{2r_h} \sqrt{w} \left[\frac{\mathfrak{b}_{xz}^{(-)}(1)}{\mathfrak{b}_{xz}^{(-)}(0)} \right]^2 \ln u \right) + \mathcal{O}(u). \quad (95)$$

By substituting this expression into the expectation value (66) of the two-form current $\langle J^{\mu\nu} \rangle$, we obtain

$$\langle \delta J^{xz} \rangle = \lim_{u \rightarrow 0} \left(2u^{3/2} \sqrt{F} \delta B'_{xz}(u) \right) = \frac{2\pi^2}{N_c^2} \left(2i\omega r_h^{-1} \sqrt{w} \left[\frac{\mathfrak{b}_{xz}^{(-)}(1)}{\mathfrak{b}_{xz}^{(-)}(0)} \right]^2 \right) \delta b_{xz} + \mathcal{O}(\omega^2). \quad (96)$$

The expression on the right-hand-side of the second equation is obtained by using the relation between $\delta B_{xz}^{(0)}$, $\delta B_{xz}^{(1)}$ and δb_{xz} in (53). Note that the dependence on the electromagnetic coupling

enters into the one-point function at order ω^2 and, thus, $\bar{\alpha}$ plays no role in the holographic formula for the resistivity; r_\perp and other first-order transport coefficients are independent of the renormalised electromagnetic coupling. Finally, using the Kubo formula for r_\perp , which is derived and presented in Eq. (A5) of Appendix A, we recover the expression presented in Eq. (87). All of the six remaining transport coefficients can be obtained by following the same procedure. We refer the reader to Appendix B for their detailed derivations.

The plots of the (dimensionless) transport coefficients η_\parallel , ζ_\parallel , r_\perp and r_\parallel as a function of $T/\sqrt{\mathcal{B}}$ are presented in Figure 2. The remaining three viscosities can easily be inferred from Eq. (87). In particular, $\eta_\perp/s = 1/(4\pi)$, $\zeta_\perp = \zeta_\parallel/4$ and $\zeta_\times = -\zeta_\parallel/2$. We note that all transport coefficients satisfy the positive entropy production bounds discussed in Section I. It is interesting that the bulk viscosity inequality $\zeta_\perp\zeta_\parallel \geq \zeta_\times^2$ is saturated, i.e. $\zeta_\perp\zeta_\parallel = \zeta_\times^2$ in the plasma studied here for all parameters of the theory.

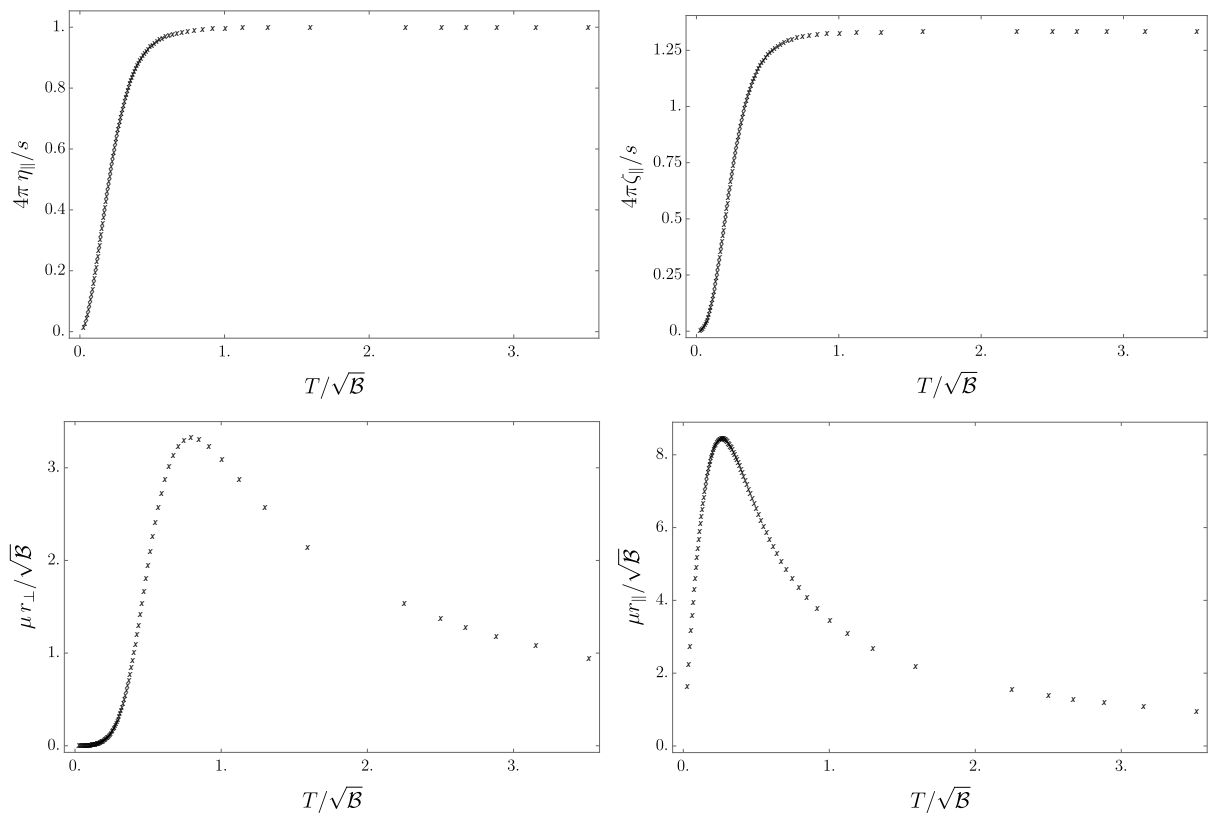


FIG. 2. The plots of (dimensionless) first-order transport coefficients as a function of $T/\sqrt{\mathcal{B}}$.

We can now investigate the behaviour of the transport coefficients in the two extreme limits of $T/\sqrt{\mathcal{B}} \rightarrow 0$ and $T/\sqrt{\mathcal{B}} \rightarrow \infty$, i.e. the strong- and the weak-field regimes, respectively. The leading-order power-law scaling (which we assume) and the coefficient follow from numerical fits. The results are presented in Table II.

Since the entropy density s vanishes in the limit of zero temperature, all first-order transport coefficients vanish in the strong-field limit of $T \rightarrow 0$. Furthermore, as we will see, all (first-order) dissipative effects also vanish in the $T \rightarrow 0$ limit. These observations are consistent with predictions

	weak field ($T/\sqrt{\mathcal{B}} \gg 1$)	strong field ($T/\sqrt{\mathcal{B}} \ll 1$)
η_{\perp}	$\frac{s}{4\pi}$	$\frac{s}{4\pi}$
η_{\parallel}	$1.00 \times \frac{s}{4\pi}$	$\frac{s}{4\pi} \left(21.32 \times \frac{T^2}{\mathcal{B}} \right)$
ζ_{\perp}	$0.33 \times \frac{s}{4\pi}$	$\frac{s}{4\pi} \left(16.34 \times \frac{T^3}{\mathcal{B}^{3/2}} \right)$
ζ_{\parallel}	$1.33 \times \frac{s}{4\pi}$	$\frac{s}{4\pi} \left(65.37 \times \frac{T^3}{\mathcal{B}^{3/2}} \right)$
ζ_{\times}	$-0.66 \times \frac{s}{4\pi}$	$-\frac{s}{4\pi} \left(32.69 \times \frac{T^3}{\mathcal{B}^{3/2}} \right)$
r_{\perp}	$\frac{\mathcal{B}}{\mu} \left(3.37 \times \frac{1}{T} \right)$	$\frac{\sqrt{\mathcal{B}}}{\mu} \left(4.7 \times \frac{T^3}{\mathcal{B}^{3/2}} \right)$
r_{\parallel}	$\frac{\mathcal{B}}{\mu} \left(3.37 \times \frac{1}{T} \right)$	$\frac{\sqrt{\mathcal{B}}}{\mu} \left(62.3 \times \frac{T}{\sqrt{\mathcal{B}}} \right)$

TABLE II. Approximate asymptotic behaviour of all first-order transport coefficients in weak- and strong-field limits. The temperature-dependent scaling of the shear viscosities at low temperature agrees with what was reported in Ref. [27].

of [22] based on symmetry arguments.

In the regime of a weak magnetic field, $T \gg \sqrt{\mathcal{B}}$, we find that both shear viscosities η_{\perp} and η_{\parallel} converge to $\eta_{\perp} = \eta_{\parallel} = s/(4\pi)$ as $\mathcal{B}/T^2 \rightarrow 0$. On the other hand, the longitudinal bulk viscosity limits to $\zeta_{\parallel} \rightarrow 4\eta/3$, which is consistent with the fact that as $\mathcal{B}/T^2 \rightarrow 0$, the evolution of the plasma should be governed by uncharged relativistic conformal hydrodynamics (see e.g. [23] or Appendix B). Indeed, both resistivities, r_{\perp} and r_{\parallel} , also tend to zero in the limit.

We also note that the weak-field behaviour of r_{\perp} and r_{\parallel} is consistent with the assumption used to construct standard (ideal) MHD, whereby conductivity is taken to infinity, $\sigma \approx 1/r \rightarrow \infty$, and whereby one adds corrections proportional to $1/\sigma$.¹⁷ In other words, small weak-field resistivities are compatible with the assumption of ideal Ohm's law, which gives rise to Eq. (7) (see also our discussion around this equation in Section I.). Furthermore, note that in standard MHD, only one resistivity (conductivity) is typically added to include dissipative corrections. What we see is that in our theory, the two resistivities take similar values in the weak-field limit in which standard MHD applies. However, in the strong-field limit, they assume drastically different values, including a different scaling with $T/\sqrt{\mathcal{B}}$. This observation therefore further points to the important role of anisotropic effects in MHD [22] and the necessity for using the formulation of [22, 25] as one moves from the weak- to the strong-field regime.

The fact that r_{\perp} and r_{\parallel} tend to zero both in the limits of $T/\sqrt{\mathcal{B}} \rightarrow 0$ and $T\sqrt{\mathcal{B}} \rightarrow \infty$, along with the positivity of the entropy production bounds $r_{\perp} \geq 0$ and $r_{\parallel} \geq 0$ [22], implies that there always exists a maximum value of the resistivities at some intermediate $T/\sqrt{\mathcal{B}}$. It would be interesting to find the sizes of these maxima in experimentally realisable systems and probe the regimes of the “least conductive” plasmas. Finally, it would be interesting to further investigate the connection between maximal r and various discussions of lower bounds on conductivities, e.g. [77–79].

¹⁷ See Ref. [22] for a discussion regarding the subtleties in relating resistivities to conductivities.

IV. MAGNETOHYDRODYNAMIC WAVES IN A STRONGLY COUPLED PLASMA

We are now ready to use the information obtained from the holographic analysis of Section III to study dissipative dispersion relations of magnetohydrodynamic waves in a toy model of a strongly coupled plasma. We will use the theory of MHD [22], which is a phenomenological effective theory, and supplement it with microscopic details—the equation of state and transport coefficients—of the holographic setup investigated above. We will be particularly interested in the dependence of the MHD modes on the angle between momentum and magnetic field, as well as the ratio between temperature and the strength of the magnetic field. The 't Hooft coupling of interactions in the matter sector is not tuneable in our model, however, the electromagnetic coupling is. In all sections, except in Section IV C, it will be set to $\alpha = 2\pi^2/137N_c^2$.

Before presenting the numerical result, we review the relevant facts about MHD modes. For a detailed derivation of these results, see Ref. [22] and for a discussion of the general procedure, see Refs. [23, 80]. First, we write the hydrodynamic variables u^μ , h^μ , T and μ in terms of oscillating modes perturbed around their near-equilibrium values, e.g. $u^\mu \rightarrow (1, 0, 0, 0) + \delta u^\mu e^{-i\omega t + ikx \sin \theta + ikz \cos \theta}$, so that $\theta \in [0, \pi/2]$ measures the angle between the equilibrium magnetic field pointing in the z -direction and the wave momentum k in the x - z plane. The dispersion relations $\omega(k)$ are then derived from the equations of MHD, i.e. Eqs. (8) and (9), with the external $H_{\mu\nu\rho} = 0$. The solutions depend on the angle θ , temperature T and the strength of the magnetic field (or the chemical potential of the magnetic flux number density), parametrised in our solutions by \mathcal{B} . Any dimensionless quantity will only depend on the single dimensionless ratio $T/\sqrt{\mathcal{B}}$. The resulting modes can be decomposed into two channels—odd and even under the reflection of $y \rightarrow -y$. The first channel is the transverse Alfvén channel. The second is the magnetosonic channel with two branches of solutions: slow and fast magnetosonic waves.

The linearised MHD equations of motion (8) and (9) need to be expanded in the hydrodynamic regime in powers of small $\omega/\Lambda_h \ll 1$ and $k/\Lambda_h \ll 1$, where Λ_h is the UV cut-off of the effective theory. In standard MHD, where $T \gg \sqrt{\mathcal{B}}$, then $\Lambda_h \approx T$, whereas in the strong-field regime of $T \ll \sqrt{\mathcal{B}}$, the cut-off can be set by the magnetic field, then $\Lambda_h \approx \sqrt{\mathcal{B}}$. As argued in [22], hydrodynamics may exist all the way to $T \rightarrow 0$, even when $\delta T = 0$. Such an expansion, performed to some order, gives rise to a polynomial equation in ω and k . For example, in the Alfvén channel, within first-order dissipative MHD,

$$-\omega^2 + \left(\frac{\mu\rho \cos^2 \theta}{\varepsilon + p}\right) k^2 - i \left[\left(\frac{\mu r_\perp}{\rho} + \frac{\eta_\parallel}{\varepsilon + p}\right) \cos^2 \theta + \left(\frac{\mu r_\parallel}{\rho} + \frac{\eta_\perp}{\varepsilon + p}\right) \sin^2 \theta \right] \omega k^2 + \frac{\mu}{2\rho(\varepsilon + p)} (r_\perp \cos^2 \theta + 2r_\parallel \sin^2 \theta) (\eta_\perp \sin^2 \theta + \eta_\parallel \cos^2 \theta) k^4 = 0. \quad (97)$$

The two solutions of the quadratic equation for ω are given by

$$\omega = -\frac{i}{2}(\mathcal{D}_{A,+})k^2 \pm \frac{k}{2}\sqrt{\mathcal{V}_A^2 \cos^2 \theta - (\mathcal{D}_{A,-})^2 k^2}, \quad (98)$$

where $\mathcal{D}_{A,+}$ and $\mathcal{D}_{A,-}$ are

$$\mathcal{D}_{A,\pm} = \left(\frac{\mu r_\perp}{\rho} \pm \frac{\eta_\parallel}{\varepsilon + p}\right) \cos^2 \theta + \left(\frac{\mu r_\parallel}{\rho} \pm \frac{\eta_\perp}{\varepsilon + p}\right) \sin^2 \theta. \quad (99)$$

One can now series expand $\omega(k) = \mathcal{D}_0 k + \mathcal{D}_1 k^2$, or alternatively, plug this ansatz in Eq. (97) and solve it order-by-order in k . What we find is the Alfvén wave dispersion relation [22]:

$$\omega = \pm \mathcal{V}_A k \cos \theta - \frac{i}{2} \left(\frac{1}{\varepsilon + p} (\eta_\perp \sin^2 \theta + \eta_\parallel \cos^2 \theta) + \frac{\mu}{\rho} (r_\perp \cos^2 \theta + r_\parallel \sin^2 \theta) \right) k^2, \quad (100)$$

where the speed is given by $\mathcal{V}_A^2 = \mu\rho/(\varepsilon + p)$. The dispersion relation appears to be well-defined for any angle $\theta \in [0, \pi/2]$ between momentum and equilibrium magnetic field. In particular, if we were to take the $\theta \rightarrow \pi/2$ limit, (100) would yield two diffusive modes, both with dispersion relation

$$\omega = -\frac{i}{2} \left(\frac{\eta_\perp}{\varepsilon + p} + \frac{\mu r_\parallel}{\rho} \right) k^2, \quad (101)$$

which are, however, unphysical and only result from an incorrect order of limits of k and θ .

As can be seen from the structure of the square-root in Eq. (98), the expansion in small k is only sensible so long as $k^2 \ll \mathcal{V}_A^2 \cos^2 \theta / (\mathcal{D}_{A,-})^2$. Hence, even for a small finite k , this expansion is inapplicable for angles θ near $\theta = \pi/2$ where $\cos \theta$ becomes very small. In fact, for

$$\mathcal{V}_A^2 \cos^2 \theta \leq (\mathcal{D}_{A,-})^2 k^2, \quad (102)$$

the propagating modes cease to exist altogether and the two modes become purely imaginary (diffusive to $\mathcal{O}(k^2)$). The transmutation of two propagating Alfvén modes into two non-propagating modes occurs when the inequality in (102) is saturated, i.e. at the critical angle θ_c when $\text{Re}[\omega] = 0$:

$$\frac{\cos(\theta_c)}{\mathcal{D}_{A,-}(\theta_c)} = \frac{k}{\mathcal{V}_A}. \quad (103)$$

In other words, the plasma exhibits propagating (sound) modes for $0 \leq \theta < \theta_c$ and non-propagating (diffusive) modes for $\theta_c < \theta \leq \pi/2$. We plot the dependence of the critical angle θ_c on $k/\sqrt{\mathcal{B}}$ and $T/\sqrt{\mathcal{B}}$ for the Alfvén waves in our model in Figure 3. What we see is that for small $k/\sqrt{\mathcal{B}}$ and small $T/\sqrt{\mathcal{B}}$, the transition to diffusive modes occurs closer to $\theta_c \approx \pi/2$. For any fixed and finite $T/\sqrt{\mathcal{B}}$, Eq. (103) indeed implies that $\theta_c \rightarrow \pi/2$ as $k \rightarrow 0$.

We note that as already pointed out in [25], the limits of $k \rightarrow 0$ and $\theta \rightarrow \pi/2$ do not commute and we obtain different results depending on which expansion ($k \approx 0$ or $\theta \approx \pi/2$) is performed first. If one first takes the limit $\theta \rightarrow \pi/2$, then Eq. (97) becomes

$$-\omega^2 - i \left(\frac{\mu r_\parallel}{\rho} + \frac{\eta_\perp}{\varepsilon + p} \right) \omega k^2 + \frac{\mu r_\parallel \eta_\perp}{\rho(\varepsilon + p)} k^4 = 0, \quad (104)$$

which instead of Eq. (101) results in two non-degenerate diffusive modes

$$\omega = -i \frac{\eta_\perp}{\varepsilon + p} k^2, \quad \omega = -i \frac{\mu r_\parallel}{\rho} k^2. \quad (105)$$

The dispersion relation (100) is therefore only sensible at a finite $T/\sqrt{\mathcal{B}}$ and infinitesimally small k/Λ_h .

In the magnetosonic channel, the story is entirely analogous to the one described for the Alfvén waves. By expanding around $k \approx 0$ first, we obtain the dispersion relation of [22]:

$$\omega = \pm v_M k - i\tau k^2, \quad (106)$$

where the speed of magnetosonic wave is given by

$$v_M^2 = \frac{1}{2} \left\{ (\mathcal{V}_A^2 + \mathcal{V}_0^2) \cos^2 \theta + \mathcal{V}_S^2 \sin^2 \theta \pm \sqrt{[(\mathcal{V}_A^2 - \mathcal{V}_0^2) \cos^2 \theta + \mathcal{V}_S^2 \sin^2 \theta]^2 + 4\mathcal{V}^4 \cos^2 \theta \sin^2 \theta} \right\}. \quad (107)$$

The functions \mathcal{V}_A , \mathcal{V}_0 , \mathcal{V}_S and \mathcal{V} appearing in (107) are

$$\mathcal{V}_A^2 = \frac{\mu\rho}{\varepsilon + p}, \quad \mathcal{V}_0^2 = \frac{s}{T\chi_{11}}, \quad \mathcal{V}_S^2 = \frac{(s - \rho\chi_{12})(s + \rho\chi_{21}) + \rho^2\chi_{11}\chi_{22}}{(\varepsilon + p)\chi_{11}}, \quad \mathcal{V}^4 = \frac{s(s - \rho\chi_{12})(s + \rho\chi_{21})}{T(\varepsilon + p)\chi_{11}^2}. \quad (108)$$

The susceptibilities are¹⁸

$$\chi_{11} = \left(\frac{\partial s}{\partial T} \right)_\rho, \quad \chi_{12} = \left(\frac{\partial s}{\partial \rho} \right)_T, \quad \chi_{21} = \left(\frac{\partial \mu}{\partial T} \right)_\rho, \quad \chi_{22} = \left(\frac{\partial \mu}{\partial \rho} \right)_T. \quad (109)$$

The two types of magnetosonic waves, corresponding to \pm solutions in (107), are known as the fast (with $+$) and the slow (with $-$) magnetosonic waves. We refer the reader to Appendix C for further details regarding the derivation of the magnetosonic modes. Each pair of the propagating slow magnetosonic modes also splits, in analogy with the Alfvén waves, into two non-propagating diffusive modes for $\theta \geq \theta_c$. The critical angle θ_c for magnetosonic modes is also defined as in the Alfvén channel: the angle at which $\text{Re}[\omega] = 0$. We plot the numerically-computed dependence of the magnetosonic θ_c on $k/\sqrt{\mathcal{B}}$ and $T/\sqrt{\mathcal{B}}$ in Fig. 3. As can be seen from the plot, the critical angles for the two types of waves are independent. However, they show similar qualitative dependence on the parameters that characterise the waves.

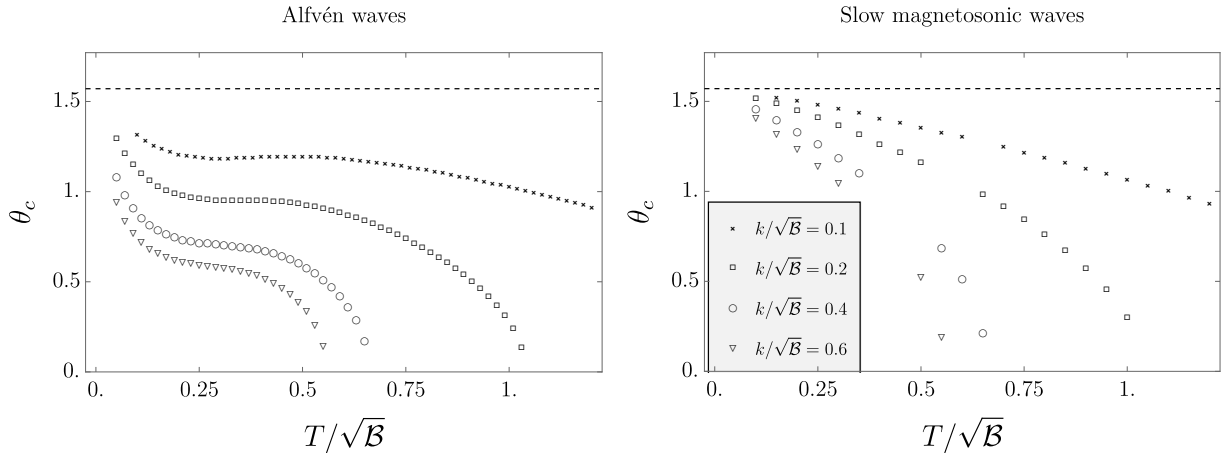


FIG. 3. The critical angle θ_c for Alfvén waves (left) and slow magnetosonic waves (right), plotted as a function of $T/\sqrt{\mathcal{B}}$ for $k/\sqrt{\mathcal{B}} = \{0.1, 0.2, 0.4, 0.6\}$. The dashed line at the top of both sub-figures indicates the value of $\theta_c = \pi/2$.

We summarise the θ -dependent characteristics of MHD modes in Fig. 4. We observe the pattern of a transmutation of sound modes into diffusion to be different in the weak- and strong-field regimes. Namely, the two magnetosonic waves interchange their dispersion relations at small

¹⁸ Note that these susceptibilities are different from the ones used in [22], where independent thermodynamic quantities were T and μ , not T and ρ . For this reason we also use different notation.

θ . Since the complicated expressions for dispersion relations greatly simplify at $\theta = 0$ and $\theta = \pi/2$, we state them below. The sound mode dispersion relations, denoted by S, are

$$\begin{aligned}
\text{S1 : } \quad \omega &= \pm \mathcal{V}_S k - \frac{i}{2} \left\{ \frac{\zeta_{\perp} + \eta_{\perp}}{\varepsilon + p} \right. \\
&\quad \left. + \frac{r_{\perp} [(s - \rho\chi_{12})(\mu - T\chi_{21}) - \rho T\chi_{11}\chi_{22}] [(s + \rho\chi_{21})(\mu + T\chi_{12}) - \rho T\chi_{11}\chi_{22}]}{T^2 \chi_{11} [(s - \rho\chi_{12})(s + \rho\chi_{21}) + \rho^2 \chi_{11}\chi_{22}]} \right\} k^2, \\
\text{S2 : } \quad \omega &= \pm \mathcal{V}_A k - \frac{i}{2} \left(\frac{\eta_{\parallel}}{\varepsilon + p} + \frac{\mu r_{\perp}}{\rho} \right) k^2, \\
\text{S3 : } \quad \omega &= \pm \mathcal{V}_0 k - \frac{i}{2} \frac{\zeta_{\parallel}}{sT} k^2,
\end{aligned} \tag{110}$$

and the diffusive modes, denoted by D, are

$$\begin{aligned}
\text{D1 : } \quad \omega &= -i \frac{\eta_{\parallel}}{sT} k^2, \\
\text{D2 : } \quad \omega &= -\frac{i r_{\perp} (\varepsilon + p)^2 \chi_{22}}{T^2 [(s - \rho\chi_{12})(s + \rho\chi_{21}) + \rho^2 \chi_{11}\chi_{22}]} k^2, \\
\text{D3 : } \quad \omega &= -i \frac{\eta_{\perp}}{\varepsilon + p} k^2, \\
\text{D4 : } \quad \omega &= -i \frac{r_{\parallel} \mu}{\rho} k^2.
\end{aligned} \tag{111}$$

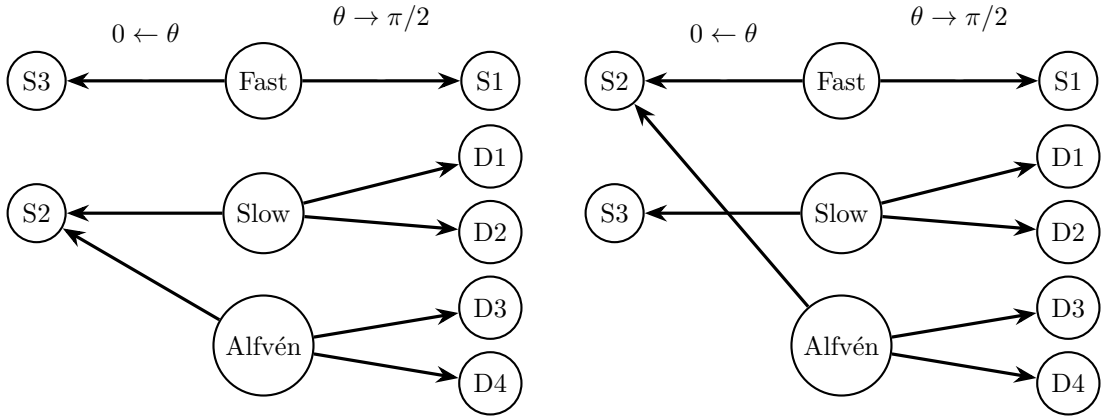


FIG. 4. Diagrams depicting the θ -dependent pattern of transmutation from sound to diffusive modes for Alfvén waves and slow and fast magnetosonic waves. The left and right diagrams correspond to weak- and strong-field regimes. The relevant dispersion relation are stated in Eqs. (110) and (111).

In the regime of a large $T/\sqrt{\mathcal{B}}$, the results agree with those of [25]. Furthermore, using the asymptotic form of the thermodynamics quantities and transport coefficients in the $T/\sqrt{\mathcal{B}} \rightarrow \infty$ limit, one can show that these modes reduce to sound and diffusive modes of uncharged relativistic hydrodynamics.

In the strong-field regime, which cannot be described within standard MHD, the speeds of S1 and S3 become large and approach the speed of light in the limit of $T \rightarrow 0$. It is clear that in

the strong-field regime, MHD sound waves can easily violate any causal upper bound on the speed of sound [81–84]. Furthermore, as discussed above, all diffusion constants vanish and the system becomes controlled by second-order MHD [22], which we do not investigate in this work. All details regarding angle-dependent wave propagation are presented in Section IV B.

A. Speeds and attenuations of MHD waves

Here, we plot the speeds (phase velocities) and first-order attenuation coefficients of the three types of MHD sound waves: the Alfvén and the fast and slow magnetosonic waves for the holographic strongly coupled plasma discussed above. These results assume an infinitesimally small value of momentum k , and follow from first expanding the polynomial equation of the type of (97) around $k \approx 0$ and writing each dispersion relation as $\omega = \pm vk - i\mathcal{D}k^2$. The speeds v (presented in Fig. 5) and attenuation coefficients \mathcal{D} (presented in Fig. 6) are then plotted for all $0 \leq \theta \leq \pi/2$, which, as discussed above, is only physically sensible when $\theta_c \rightarrow \pi/2$, i.e. as $k \rightarrow 0$.

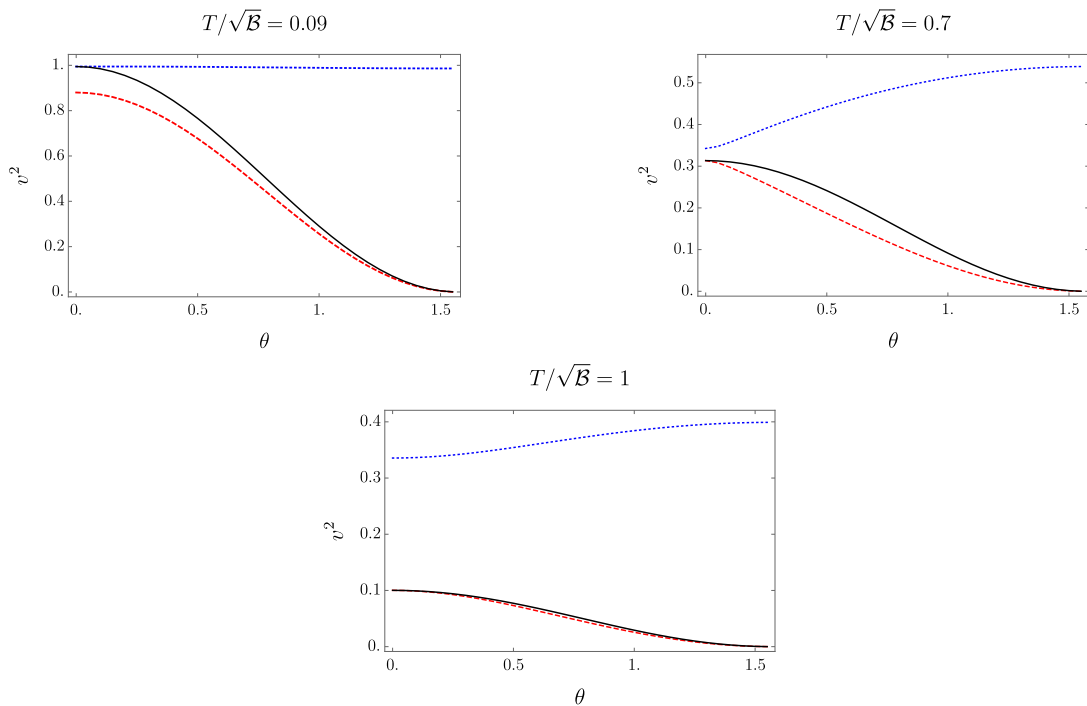


FIG. 5. Angular dependence of the speeds of Alfvén (black, solid), fast (blue, dotted) and slow (red, dashed) magnetosonic waves in the strong-field, the crossover and the weak-field regimes.

The angular profiles of the speeds and the dissipative attenuation coefficients show distinct behaviour in the strong-, the crossover (cf. Eq. (85)) and the weak-field regimes. In particular, the speeds of sound enter the weak-field regime, where they reduce to well-known standard MHD results, rapidly after the temperature exceeds $T/\sqrt{\mathcal{B}} \approx 0.7$. There, Alfvén and slow magnetosonic waves travel with very similar speeds for all θ and their speeds coincide at $\theta = 0$ and $\theta = \pi/2$. The situation is different in the strong-field regime where the profiles of speeds qualitatively match the strong-field predictions of [22]. There, slow magnetosonic and Alfvén waves can travel faster at

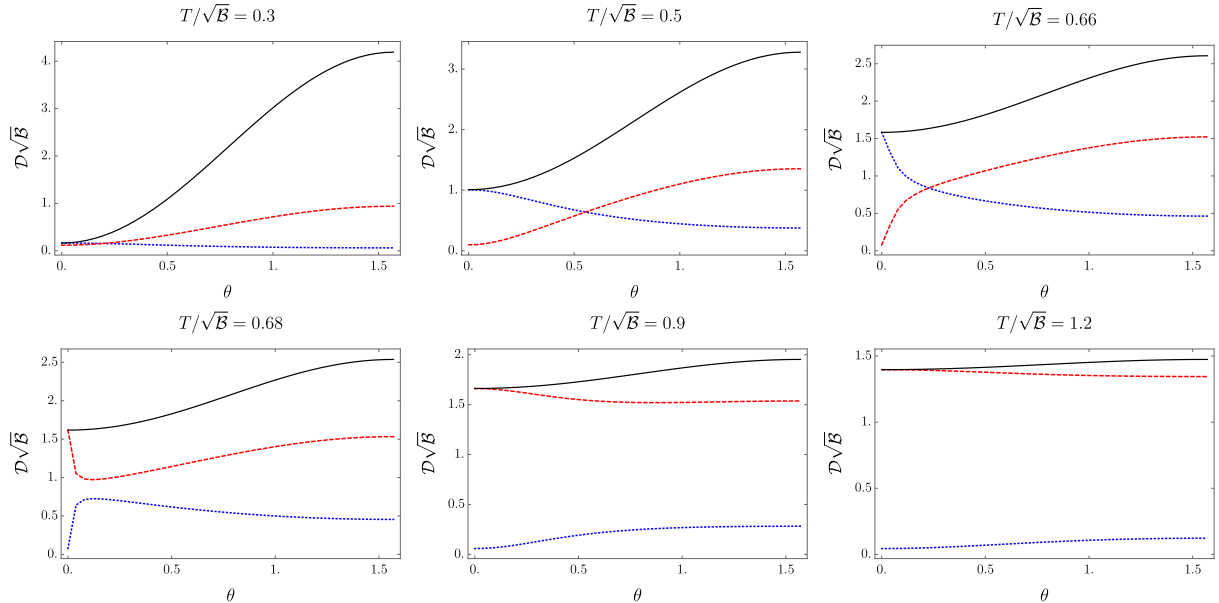


FIG. 6. Angular dependence of the (dimensionless) attenuation coefficients of Alfvén (black, solid), fast (blue, dotted) and slow (red, dashed) magnetosonic waves, $\mathcal{D}\sqrt{\mathcal{B}}$, in the strong-field, the crossover and the weak-field regimes.

small θ , with speeds comparable to those of fast magnetosonic waves. At $\theta = 0$, the Alfvén speed equals that of fast, instead of slow, magnetosonic waves (cf. Fig. 4). It should also be noted that there exists a value of $T/\sqrt{\mathcal{B}}$ in the crossover regimes where all three speeds are equal at $\theta = 0$.

The attenuation coefficients, computed with all seven transport coefficients [22, 25], are computed for the first time for a concrete microscopically (holographically) realisable plasma and therefore difficult to compare with other past results. What we observe is that the Alfvén waves experience the strongest damping for all values of $T/\sqrt{\mathcal{B}}$. Beyond that, the qualitative behaviour again displays distinct angle-dependent features in the three regimes, which are apparent from Fig. 6. A noteworthy, but not a surprising fact is that the strength of attenuation appears to be much more strongly dependent on the angle between momentum and magnetic field in the regime of small $T/\sqrt{\mathcal{B}}$. Furthermore, in the crossover regime, we find that the strengths of fast and slow magnetosonic mode attenuations interchange roles as $T/\sqrt{\mathcal{B}}$ increases. In plots at $T/\sqrt{\mathcal{B}} = 0.5$ and $T/\sqrt{\mathcal{B}} = 0.66$, there exists an angle θ at which the two attenuation strengths coincide.

B. MHD modes on a complex frequency plane

By assuming a finite value of momentum k , a full analysis of the spectrum requires us to take into account the transmutation of sound modes into non-propagating diffusive modes. The pattern of this behaviour, as a function of the angle between momentum and the direction of the equilibrium magnetic field θ , was summarised in Fig. 4. Motivated by holographic quasinormal mode (poles of two-point correlators) analyses, we plot the motion of the MHD modes on the complex frequency plane—here, as a function of θ and $T/\sqrt{\mathcal{B}}$. One should consider these plots as a prediction of

how the first-order approximation to the hydrodynamic sector of the full quasinormal spectrum computed from the theory (42) is expected to behave.

In Fig. 7, we plot the typical θ -dependent trajectories of $\omega(\theta)$ for Alfvén and magnetosonic modes in distinctly strong- and weak-field regimes. At all temperatures (except at $T = 0$ where $\mathcal{D} = 0$), the behaviour is consistent with our previous discussions, including the fact that the transmutation of Alfvén and slow magnetosonic waves into diffusive modes occurs at lower θ_c as $k/\sqrt{\mathcal{B}}$ increases.

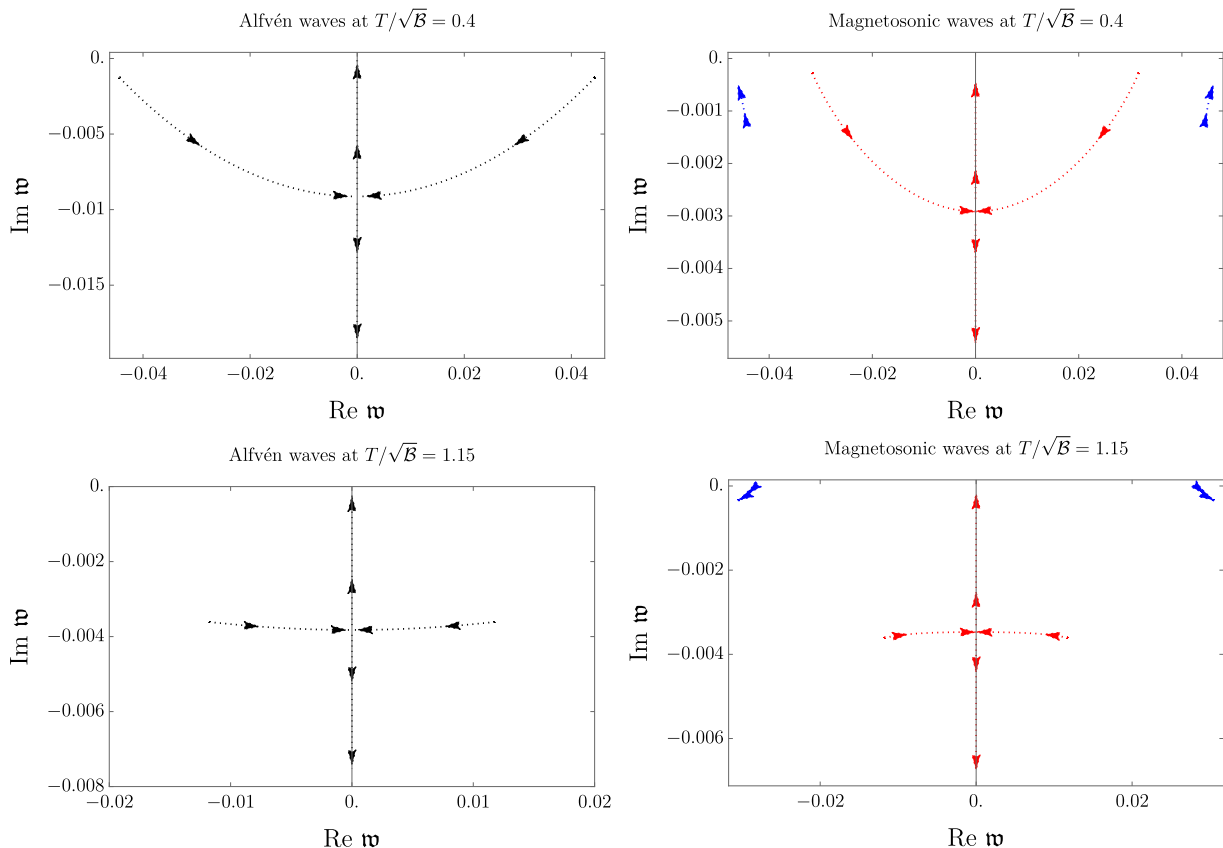


FIG. 7. Dependence of the complex (dimensionless) frequency $\mathfrak{\omega} = \omega/\sqrt{\mathcal{B}}$ on θ , plotted for Alfvén (black) and fast (blue) and slow (red) magnetosonic waves in the strong- and weak-field regimes with $T/\sqrt{\mathcal{B}} = 0.4$ and $T/\sqrt{\mathcal{B}} = 1.15$, respectively. The arrows represent the motion of poles as θ is tuned from 0 to $\pi/2$. Momentum is set to $k/\sqrt{\mathcal{B}} = 0.05$.

In the crossover temperature regime (around $T/\sqrt{\mathcal{B}} \approx 0.6$), we can observe in more detail the interplay between fast and slow magnetosonic modes, which was noted in Section IV A. While the speed of fast magnetosonic waves always exceeds that of slow waves, their attenuation strengths exchange roles around $T/\sqrt{\mathcal{B}} \approx 0.675$, which manifests in a characteristically distinct behaviour for $\theta < \theta_c$, presented in Fig. 8 (see also Fig. 6). The θ -dependence of Alfvén waves remains qualitatively similar to those depicted in Fig. 7.

For a fixed $\theta < \theta_c$, where θ_c depends on k and $T/\sqrt{\mathcal{B}}$, we plot the typical behaviour of $\omega(k)$ as a function of $T/\sqrt{\mathcal{B}}$ in Fig. 9. At $T = 0$, all poles start from the non-dissipative regime (the real $\mathfrak{\omega}$ axis), with the speed of fast magnetosonic waves given by $v = 1$. As they move

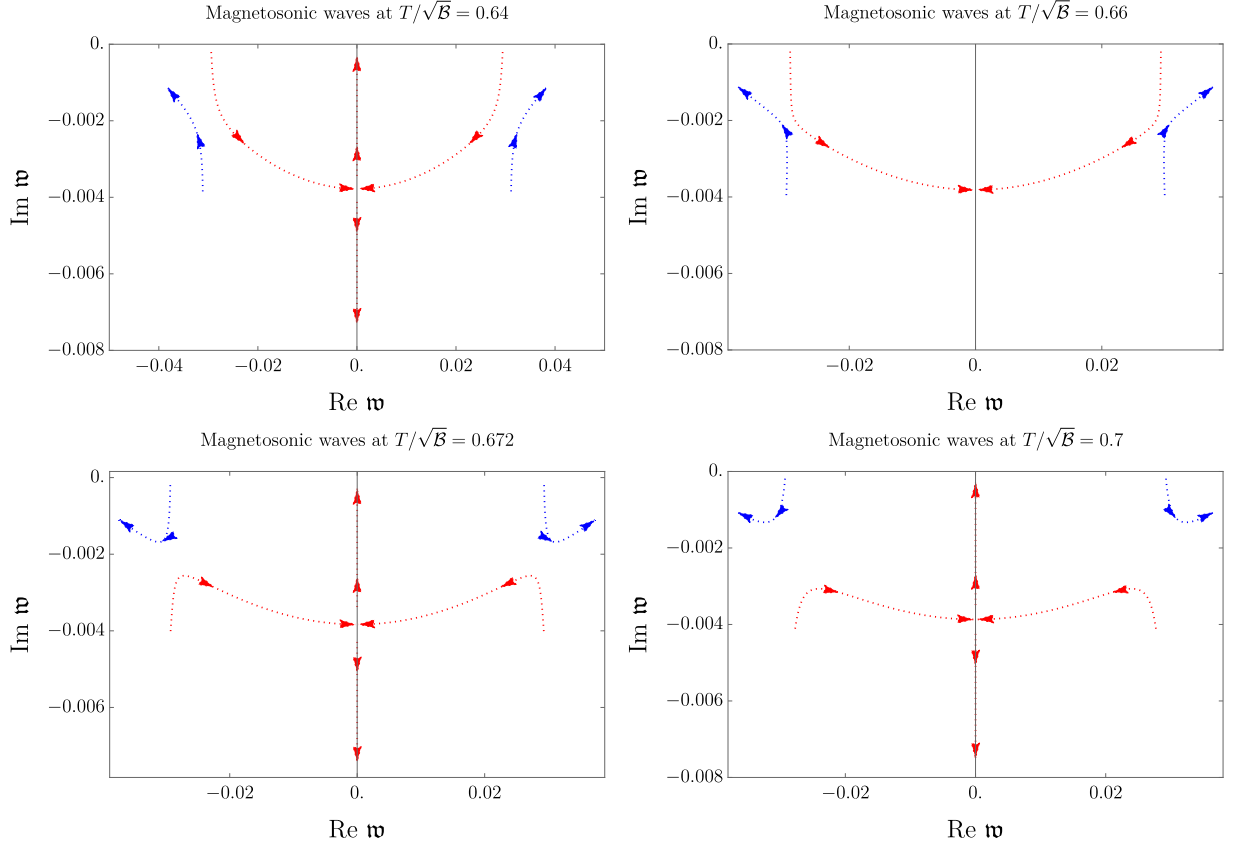


FIG. 8. Dependence of the complex (dimensionless) frequency $\mathfrak{w} = \omega/\sqrt{\mathcal{B}}$ of fast (blue) and slow (red) magnetosonic modes on θ in the crossover regime. The arrows represent the motion of poles as θ is tuned from 0 to $\pi/2$. Momentum is set to $k/\sqrt{\mathcal{B}} = 0.05$.

towards larger $T/\sqrt{\mathcal{B}}$, the Alfvén and the slow magnetosonic modes again asymptote to each other, eventually transforming into diffusive modes, while the speed of the fast magnetosonic modes gradually converges towards that of neutral conformal sound with $v = 1/\sqrt{3}$.

In the high temperature limit, the “collision” of the Alfvén and, independently, the slow magnetosonic poles on the imaginary axis occurs close to the real axis, which follows from the fact that for both types of waves,

$$\text{Im}[\mathfrak{w}] \approx -\frac{1}{2} \left(\frac{\eta}{\varepsilon + p} + \frac{\mu r}{\mathcal{B}} \right) \sqrt{\mathcal{B}} \sim -\frac{\sqrt{\mathcal{B}}}{T} \rightarrow 0, \quad (112)$$

as $T/\sqrt{\mathcal{B}} \rightarrow \infty$. The Alfvén waves then become the diffusive modes of uncharged conformal hydrodynamics with $\omega = -i\eta k^2/(2sT)$. As for our final plot, in Fig. 10, we present the dependence of the four diffusion constants and one sound attenuation coefficient on the temperature at $\theta = \pi/2$ (cf. Fig. 4 and Eqs. (110)–(111)). The modes D1, D3 and S1 reduce to dispersion relations of uncharged relativistic hydrodynamics. D2 and D4 are new.

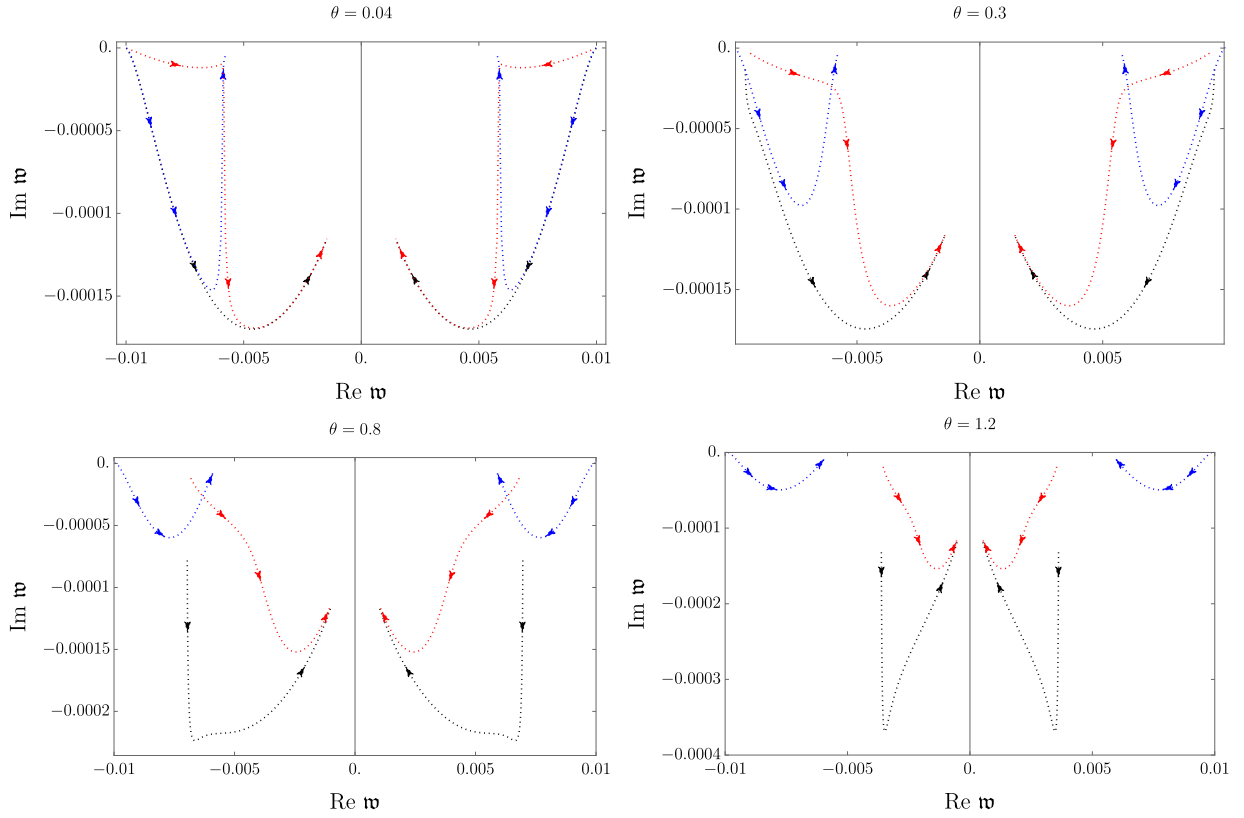


FIG. 9. Dependence of the complex (dimensionless) frequency $\mathfrak{w} = \omega/\sqrt{\mathcal{B}}$ on $T/\sqrt{\mathcal{B}}$, plotted for Alfvén (black) and fast (blue) and slow (red) magnetosonic waves for $\theta < \theta_c$. The arrows represent the motion of poles as $T/\sqrt{\mathcal{B}}$ is tuned from 0 towards the weak-field regime. Momentum is set to $k/\sqrt{\mathcal{B}} = 0.01$.

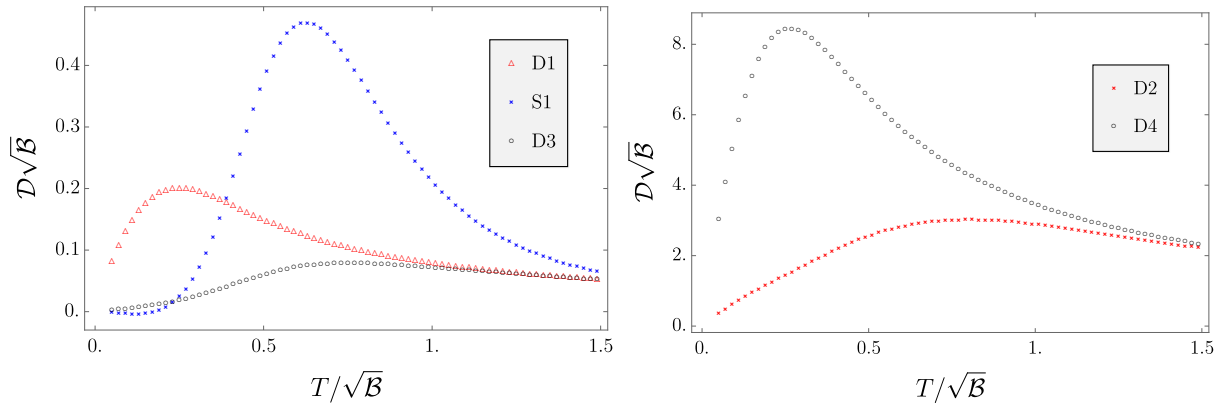


FIG. 10. Plots of the four diffusion constants (D1, D2, D3, D4) and the sound attenuation (S1) as a function of $T/\sqrt{\mathcal{B}}$ at $\theta = \pi/2$. Black, red and blue curves depict dissipative coefficients that originate from the Alfvén, slow magnetosonic and fast magnetosonic waves, respectively.

C. Electric charge dependence

We end our discussion of MHD dispersion relations by investigating their dependence on the choice of the $U(1)$ coupling constant, which has so far been set to the (N_c -rescaled) $\bar{\alpha} = 1/137$.

All dependence on $\bar{\alpha}$ enters into the expectation value of the stress-energy tensor through the term proportional to $\mathcal{H}_{\mu\nu}\mathcal{H}^{\mu\nu}\ln\mathcal{C}$ (cf. Eq. (65)), which contributes no terms linear in ω . For this reason, while the equation of state strongly depends on $\bar{\alpha}$, the first-order transport coefficients do not. Hence, all speeds of sound and attenuation (and diffusive) coefficients depend on the choice of $\bar{\alpha}$ through the equation of state and susceptibilities.

What we observe is that the speeds of waves and attenuation coefficients strongly depend on the renormalised electromagnetic coupling, so, unsurprisingly, the strength of electromagnetic interactions plays an important role in the phenomenology of MHD. For concreteness, we only present the detailed behaviour of the Alfvén waves (with speed $\mathcal{V}_A \cos\theta$), which reduce to the neutral hydrodynamic diffusive mode D3 (and D4) at $\theta = \pi/2$. Both \mathcal{V}_A and the diffusion constant of D3, \mathcal{D}_{D3} , strongly depend on $\bar{\alpha}$. For a small variation in the values of $\bar{\alpha}$, we plot the results in Fig. 11.¹⁹ To show the importance of a sensible choice of the renormalisation condition, we also vary the coupling over a larger range (to $\bar{\alpha} = 80/137$), where we see that the system develops unphysical behaviour with instabilities. As is apparent from Fig. 12, Alfvén waves become unstable at low $T/\sqrt{\mathcal{B}}$.

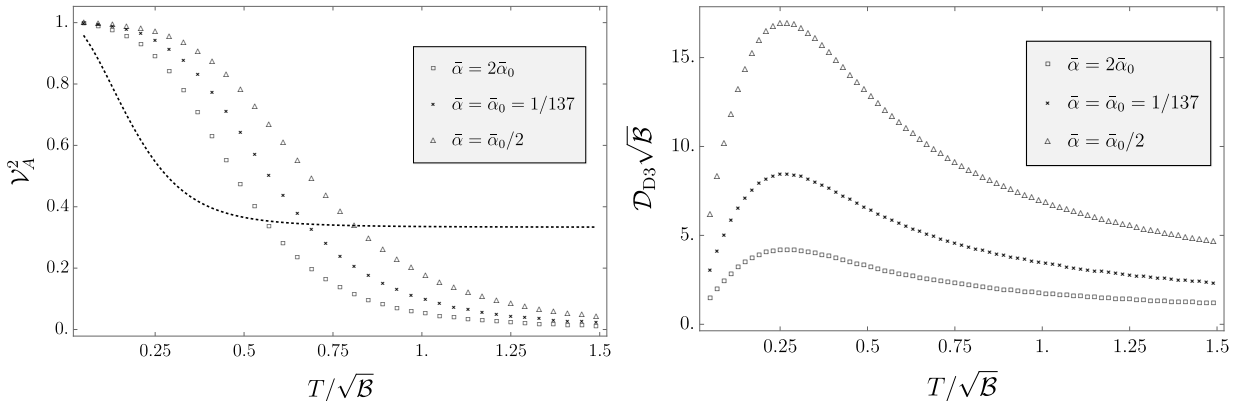


FIG. 11. The plot of \mathcal{V}_A^2 and the diffusion constant \mathcal{D}_{D3} at $\bar{\alpha} = \{\bar{\alpha}_0/2, \bar{\alpha}_0, 2\bar{\alpha}_0\}$, where $\bar{\alpha}_0 = 1/137$. The dashed line in the left plot is the $\bar{\alpha}$ -independent speed (squared) of the S3 mode (cf. Fig. 4), i.e. \mathcal{V}_0^2 , which is plotted for comparison.

In all to us known literature, the unavoidable choice of the constant \mathcal{C} , which sets $\bar{\alpha}$, is made in a different way. \mathcal{C} is either chosen so that the logarithmic terms vanish altogether, or so that it sets the UV scale to that of the magnetic field, which is convenient when studying strong magnetic fields as e.g. in [36, 45]. Here, we wish to point out some of the consequences of setting \mathcal{C} to either of the two standard options. The first option, which eliminates the logarithmic terms, results in the following thermodynamics quantities:

$$\varepsilon = \frac{N_c^2}{2\pi^2} \left(-\frac{3}{4} f_4^b r_h^4 \right), \quad p = \frac{N_c^2}{2\pi^2} \left[\left(-\frac{1}{4} f_4^b + \frac{v_4^b}{v} \right) r_h^4 - \frac{\mathcal{B}^2}{4} \right], \quad \mu\rho = \frac{N_c^2}{2\pi^2} \left(\frac{3v_4^b}{v} r_h^4 - \frac{\mathcal{B}^2}{4} \right). \quad (113)$$

¹⁹ We remind the reader that in the boundary Lagrangian, the electromagnetic coupling is scaled out from the covariant derivatives. Thus, only the Maxwell term depends on e_r . As we vary e_r , we keep the strength of the electromagnetic field fixed.

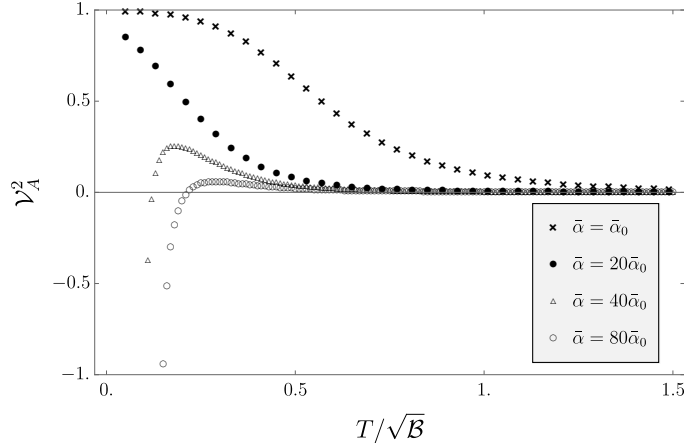


FIG. 12. The plot of the Alfvén \mathcal{V}_A^2 at a varying $\bar{\alpha}$ ranging from $\bar{\alpha} = \bar{\alpha}_0$ to $\bar{\alpha} = 80\bar{\alpha}_0$, where $\bar{\alpha}_0 = 1/137$. We see that as $\bar{\alpha}$ increases, the waves develop an instability in the strong-field regime.

The second choice results in

$$\begin{aligned} \varepsilon &= \frac{N_c^2}{2\pi^2} \left(-\frac{3}{4} f_4^b r_h^4 + \frac{\mathcal{B}^2}{4} \ln \mathcal{B} \right), & p &= \frac{N_c^2}{2\pi^2} \left[\left(-\frac{1}{4} f_4^b + \frac{v_4^b}{v} \right) r_h^4 - \frac{\mathcal{B}^2}{4} + \frac{\mathcal{B}^2}{4} \ln \mathcal{B} \right], \\ \mu\rho &= \frac{N_c^2}{2\pi^2} \left(\frac{3v_4^b}{v} r_h^4 - \frac{\mathcal{B}^2}{4} - \frac{\mathcal{B}^2}{4} \ln \mathcal{B} \right). \end{aligned} \quad (114)$$

While these two renormalisation conditions are suitable for studying certain physical setups involving static electromagnetic fields, we claim that they lead to unphysical results when the boundary $U(1)$ gauge field is dynamical. By comparing the renormalised stress-energy tensor (77)–(79) to expressions in (113) and (114), we find that the two choices correspond to the renormalised coupling being $e_r^2 \rightarrow \infty$ and $e_r^2 \sim \ln \mathcal{B}$, respectively. An infinite $U(1)$ coupling is unphysical in a plasma state. The problem with the second choice is that if extrapolated to the weak-field regime, $\ln \mathcal{B}/M$, where M is some scale, can become negative and e_r imaginary, which is again unphysical. Thus, these choices may lead to instabilities and superluminal propagation, which were absent from our results with $\bar{\alpha}$ near $1/137$. We plot the Alfvén speed parameter \mathcal{V}_A for the two couplings from (113) and (114) in Fig. 13.

V. DISCUSSION

This work should be considered as the first holographic step in a long road towards a better understanding of magnetohydrodynamics in plasmas outside of the regime of validity of standard MHD, be it in the presence of strong magnetic fields or in a strongly interacting (or dense) plasma with a complicated equation of state and transport coefficients—all claimed to be describable within the recent (generalised global) symmetry-based formulation of MHD of Ref. [22]. In order to supply a hydrodynamical theory of MHD with the necessary microscopic information of a strongly coupled plasma, we resorted to the simplest, albeit experimentally inaccessible option: holography. Nevertheless, our hope is that in analogy with the myriad of works on holographic conformal hydrodynamics, which have led to important new insights into strongly interacting realistic fluids,

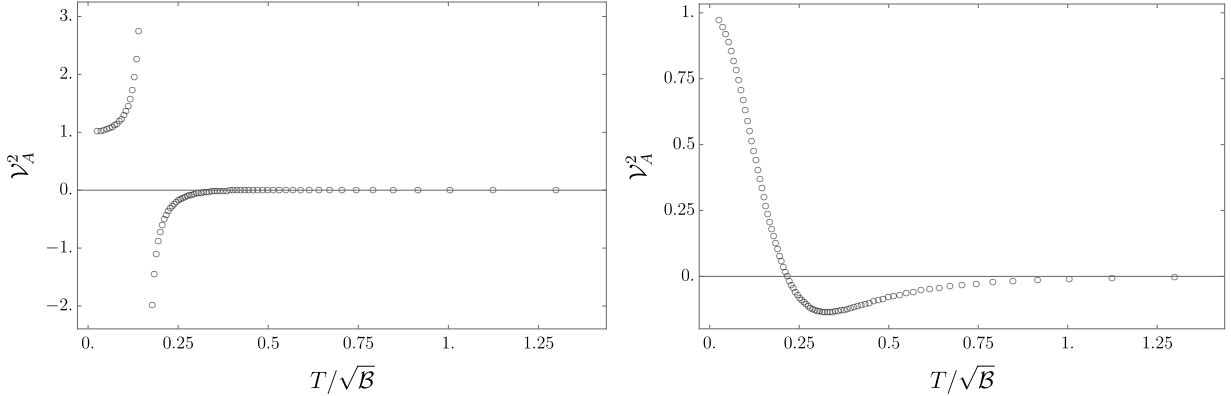


FIG. 13. The θ -independent factor \mathcal{V}_A of the Alfvén wave speed plotted for the renormalised $e_r^2 \rightarrow \infty$ (left) from Eq. (113) and for $e^2 \sim \ln \mathcal{B}$ (right) from Eq. (114).

holography can also help us understand observable MHD states in the presence of strong fields, high density and of strongly interacting gauge theories, such as QCD.

With this view, we constructed the simplest theory dual to the operator structure and Ward identities used in MHD of [22], investigated the relevant aspects of the holographic dictionary and used it to compute the equation of state and transport coefficients of the dual plasma state. This information was then used to analyse the dependence of MHD waves—Alfvén and magnetosonic waves—on tuneable parameters specifying the state: the strength of the magnetic field, temperature, the angle between momentum of propagation and the equilibrium magnetic field direction, as well as the strength of the $U(1)$ electromagnetic gauge coupling. We believe that the latter feature of our model—dynamical electromagnetism on the boundary—which in the (dual) language of two-form gauge fields in the bulk allows for standard (Dirichet) quantisation, could in its own right be used for holographic studies of $U(1)$ -gauge systems, unrelated to MHD.

Our results have revealed several new qualitative features of MHD waves, particularly in the regime of a strong magnetic field, which is inaccessible to standard MHD methods. Various properties of the equation of state, transport coefficients and dispersion relations found here, may now be compared to those in experimentally realisable plasmas, or at the least, used as a toy model for future studies of MHD. Approximate scalings in the limiting regimes of large and small $T/\sqrt{\mathcal{B}}$ are collected in Tables I and II. Here, we summarise some of the most interesting observations:

- The equation of state and transport coefficients strongly depend on the strength of the magnetic field, i.e. on whether the plasma is in the weak-field, the crossover, or the strong-field regime.
- In the weak-field regime with $T/\sqrt{\mathcal{B}} \gg 1$, the system is well-described by standard MHD (see [25] for a full description) with small resistivities (large conductivity regime, which is assumed by ideal Ohm’s law) and small effects of anisotropy. As $T/\sqrt{\mathcal{B}} \rightarrow \infty$, the plasma becomes an uncharged, conformal fluid with a single independent transport coefficient, $\eta = s/4\pi$. In the strong-field limit of $T/\sqrt{\mathcal{B}} \rightarrow 0$, the plasma limits to a non-dissipative regime with all first-order transport coefficients (along with sound attenuations and diffusion constants) tending to zero. Effects of anisotropy are large.

- Resistivities have a global maximum in the intermediate $T/\sqrt{\mathcal{B}}$ regime, which indicates a regime of least conductive plasma. If the assumptions of standard MHD are correct at $T/\sqrt{\mathcal{B}} \gg 1$ and the symmetry-based predictions of [22] are correct at $T/\sqrt{\mathcal{B}} \ll 1$, such a regime should be generically exhibited by any plasma.

- Out of the three bulk viscosities, ζ_{\perp} , ζ_{\parallel} and ζ_{\times} , only one is independent and they saturate the positivity of the entropy production inequality, i.e. they are related by $\zeta_{\perp}\zeta_{\parallel} = \zeta_{\times}^2$. One may speculate on how general this result is and whether it is related to the suppression of entropy production at strong coupling [85, 86] or perhaps some form of (holographic) universality at infinite (or strong) coupling.

- Various qualitative features of slow and fast magnetosonic modes are exchanged in the weak- and strong-field regimes (usually at small angles, θ , between momentum and the equilibrium magnetic field direction), such as their asymptotic tendency to the speed of Alfvén waves and the strength of sound attenuation.

- For a finite momentum, propagating Alfvén and slow magnetosonic modes (sound modes to $\mathcal{O}(k^2)$) transmute into pairs of non-propagating, diffusive (to $\mathcal{O}(k^2)$) modes. This occurs at large angles between the direction of momentum propagation and the equilibrium magnetic field, $\theta_c < \theta \leq \pi/2$, where θ_c is some momentum- and $T/\sqrt{\mathcal{B}}$ -dependent critical angle (cf. Eq. (103) for Alfvén waves).

- The phenomenology of MHD modes strongly depends on the strength of the electromagnetic coupling and can, for large ranges of the coupling, lead to unstable or superluminal propagation.

Beyond the types of waves studied in this work, it would be particularly interesting to better understand the role of finite charge density, as studied in [25], within the formalism of [22]. The important question then is how the phenomenology of such MHD waves, which typically experience gapped propagation and instabilities (e.g. the infamous Weibel instability), becomes altered by strong interactions, strong fields and for more ‘exotic’ field content.

Finally, the holographic setup studied here will need to undergo extensive further tests and analyses in order to unambiguously establish its connection to plasma physics and MHD. In particular, it is essential to study the quasinormal spectrum of the theory to verify that the hydrodynamic modes indeed describe the small- ω and small- k expansion of the leading infrared poles. Furthermore, it will be interesting to understand the role of higher-frequency spectrum and its interplay with MHD modes. We leave all these and many other interesting questions to the future.

ACKNOWLEDGMENTS

The authors would like to thank Debarghya Banerjee, Pavel Kovtun, Alexander Krikun, Chris Rosen, Koenraad Schalm, Andrei Starinets, Giorgio Torrieri, Vincenzo Scopelliti, Phil Szepletowski and Jan Zaanen for stimulating discussions, and Simon Gentle for his comments on the draft of this paper. We are also grateful to Diego Hofman and Nabil Iqbal for numerous discussions on the topic of this work, comments on the manuscript and for sharing the draft of [35] prior to publication. S. G. is supported in part by a VICI grant of the Netherlands Organisation for

Scientific Research (NWO), and by the Netherlands Organisation for Scientific Research/Ministry of Science and Education (NWO/OCW). The work of N. P. is supported by the DPST scholarship from the Thai government and by Leiden University.

Appendix A: Kubo formulae for first-order transport coefficients

In this appendix, we outline the derivation of the Kubo formulae that have been used to compute the seven first-order transport coefficients of (12) (or Eqs. (14)–(19)) in Section III D [22, 25]. We derive the Kubo formulae by using the variational background field method (see e.g. [23] for a review), which amounts to varying the background metric $g_{\mu\nu}$ and background two-form gauge field $b_{\mu\nu}$, sourcing $T^{\mu\nu}$ and $J^{\mu\nu}$, by writing

$$g_{\mu\nu} \rightarrow \eta_{\mu\nu} + \int \frac{d\omega}{2\pi} e^{-i\omega t} \delta h_{\mu\nu}(\omega), \quad b_{\mu\nu} \rightarrow b_{\mu\nu}^{\text{eq}} + \int \frac{d\omega}{2\pi} e^{-i\omega t} \delta b_{\mu\nu}(\omega), \quad (\text{A1})$$

where $\delta h_{\mu\nu}$ and $\delta b_{\mu\nu}$ are small variation, $\eta_{\mu\nu}$ is the flat Minkowski metric and $b_{\mu\nu}^{\text{eq}} = 0$ (no external equilibrium source). These variations of background fields can be viewed as a sources that generate a variation in the hydrodynamic variables T , ρ (which we use here instead of μ in [22]), u^μ and h^μ :

$$T(t) \rightarrow T + \delta T(t), \quad \rho \rightarrow \rho + \delta\rho(t), \quad u^\mu \rightarrow u_{\text{eq}}^\mu + \delta u^\mu(t), \quad h^\mu \rightarrow h_{\text{eq}}^\mu + \delta h^\mu(t), \quad (\text{A2})$$

where we choose the equilibrium configuration to be $u_{\text{eq}}^\mu = \delta_t^\mu$ and $h_{\text{eq}}^\mu = \delta_z^\mu$. The normalisation and orthogonality conditions for the two vectors ($u_\mu u^\mu = -1$, $h_\mu h^\mu = 1$, $u_\mu h^\mu = 0$) imply

$$\delta u^t = \frac{1}{2} \delta h_{tt}, \quad \delta h^t = \delta u^z + \delta h_{tz}, \quad \delta h^z = -\frac{1}{2} \delta h_{zz}. \quad (\text{A3})$$

After writing δT , $\delta\rho$, δu^μ and δh^μ in terms of $\delta h_{\mu\nu}$ and $\delta b_{\mu\nu}$, we can insert these solution into

$$\mathcal{T}^{\mu\nu} \equiv \sqrt{-g} \langle T^{\mu\nu} \rangle|_{g,b}, \quad \mathcal{J}^{\mu\nu} \equiv \sqrt{-g} \langle J^{\mu\nu} \rangle|_{g,b}, \quad (\text{A4})$$

which give

$$\begin{aligned} \text{Im } \mathcal{T}^{xx} + \text{Im } \mathcal{T}^{yy} &= \omega \zeta_\perp (\delta h_{xx} + \delta h_{yy}) + \omega \zeta_\times^{(1)} \delta h_{zz} + \mathcal{O}(\omega^2, \delta h^2, \delta b^2), \\ \text{Im } \mathcal{T}^{zz} &= \frac{1}{2} \omega \zeta_\parallel \delta h_{zz} + \frac{1}{2} \omega \zeta_\times^{(2)} (\delta h_{xx} + \delta h_{yy}) + \mathcal{O}(\omega^2, \delta h^2, \delta b^2), \\ \text{Im } \mathcal{T}^{xy} &= \omega \eta_\perp \delta h_{xy} + \mathcal{O}(\omega^2, \delta h^2, \delta b^2), \\ \text{Im } \mathcal{T}^{xz} &= \omega \eta_\parallel \delta h_{xz} + \mathcal{O}(\omega^2, \delta h^2, \delta b^2), \\ \text{Im } \mathcal{J}^{xy} &= 2\omega r_\parallel \delta b_{xy} + \mathcal{O}(\omega^2, \delta h^2, \delta b^2), \\ \text{Im } \mathcal{J}^{xz} &= 2\omega r_\perp \delta b_{xz} + \mathcal{O}(\omega^2, \delta h^2, \delta b^2), \end{aligned} \quad (\text{A5})$$

where we have not imposed the Onsager relation equating $\zeta_\times^{(1)}$ with $\zeta_\times^{(2)}$ [22, 25]. By using the linear response formulae relating the variations of one-point functions to retarded two-point Green's functions,

$$\begin{aligned} \delta \mathcal{T}^{\mu\nu}(\omega, \mathbf{k}) &= -\frac{1}{2} G_{TT}^{\mu\nu, \lambda\sigma}(\omega, \mathbf{k}) \delta h_{\lambda\sigma}(\omega, \mathbf{k}) - \frac{1}{2} G_{TJ}^{\mu\nu, \lambda\sigma}(\omega, \mathbf{k}) \delta b_{\lambda\sigma}(\omega, \mathbf{k}) + \mathcal{O}(\delta h^2, \delta b^2), \\ \delta \mathcal{J}^{\mu\nu}(\omega, \mathbf{k}) &= -\frac{1}{2} G_{JT}^{\mu\nu, \lambda\sigma}(\omega, \mathbf{k}) \delta h_{\lambda\sigma}(\omega, \mathbf{k}) - G_{JJ}^{\mu\nu, \lambda\sigma}(\omega, \mathbf{k}) \delta b_{\lambda\sigma}(\omega, \mathbf{k}) + \mathcal{O}(\delta h^2, \delta b^2), \end{aligned} \quad (\text{A6})$$

it is then easy to extract the relevant Kubo formulae for the seven transport coefficients [22, 25], which we used in this work:

$$\eta_{\parallel} = \lim_{\omega \rightarrow 0} \frac{G_{TT}^{xz, xz}(\omega, 0)}{-i\omega}, \quad \eta_{\perp} = \lim_{\omega \rightarrow 0} \frac{G_{TT}^{xy, xy}(\omega, 0)}{-i\omega}, \quad (\text{A7})$$

$$\zeta_{\parallel} = \lim_{\omega \rightarrow 0} \frac{G_{TT}^{zz, zz}(\omega, 0)}{-i\omega}, \quad \zeta_{\perp} + \eta_{\perp} = \lim_{\omega \rightarrow 0} \frac{G_{TT}^{xx, xx}(\omega, 0)}{-i\omega}, \quad (\text{A8})$$

as well as

$$\zeta_{\times} = \lim_{\omega \rightarrow 0} \frac{G_{TT}^{zz, xx}(\omega, 0)}{-i\omega} = \lim_{\omega \rightarrow 0} \frac{G_{TT}^{xx, zz}(\omega, 0)}{-i\omega}. \quad (\text{A9})$$

and

$$r_{\parallel} = \lim_{\omega \rightarrow 0} \frac{G_{JJ}^{xy, xy}(\omega, 0)}{-i\omega}, \quad r_{\perp} = \lim_{\omega \rightarrow 0} \frac{G_{JJ}^{xz, xz}(\omega, 0)}{-i\omega}. \quad (\text{A10})$$

Appendix B: Further details regarding the derivation of the transport coefficients

Here, we show the details of the derivation of horizon formulae of all remaining transport coefficient: η_{\perp} , η_{\parallel} , ζ_{\perp} , ζ_{\parallel} , ζ_{\times} and r_{\parallel} . The computation are analogous to the calculation of r_{\perp} in Section III D.

(i) Shear viscosity η_{\perp}

The only relevant bulk fluctuation for η_{\perp} is δG_{xy} with the equation of motion

$$\delta G_x^{y''} + \left(\frac{3}{2u} + \frac{F'}{F} + 2\mathcal{V}' + \mathcal{W}' \right) \delta G_x^{y'} + \frac{\omega^2}{4r_h^2 u^3 F^2} \delta G_x^y = 0. \quad (\text{B1})$$

The solution to leading order in the frequency ω can be found analytically and its near-boundary expansion gives

$$\delta G_x^y = \delta h_{xy} \left(1 + \frac{i\omega u^2}{4r_h v \sqrt{w}} + \mathcal{O}(u^3) \right), \quad (\text{B2})$$

where δh_{xy} is the Dirichlet background condition and the boundary theory source. If we plug this solution into to the stress-energy tensor, we find that

$$\begin{aligned} \langle \delta T^{xy} \rangle &= \frac{N_c^2}{2\pi^2} \left(\frac{r_h^4 e^{2\mathcal{V}} \sqrt{uF}}{2v} \delta G_x^{y'} \right) + \dots \\ &= \frac{N_c^2}{2\pi^2} \left(\frac{i\omega r_h^3}{4v \sqrt{w}} \right) \delta h_{xy} + \dots, \end{aligned} \quad (\text{B3})$$

Using Eq. (A5), we find that

$$\eta_{\perp} = \frac{N_c^2}{2\pi^2} \left(\frac{r_h^3}{4v \sqrt{w}} \right) = \frac{1}{4\pi} s, \quad (\text{B4})$$

as stated in Eq. (87).

(ii) *Shear viscosity* η_{\parallel}

Similarly to the computation of r_{\perp} , the xu -component of the two-form gauge field fluctuation equation can be used to reduced the two coupled second order differential equations coupling δG_{xz} and δB_{tx} to a single equation:

$$\delta G_{xz}'' + \left(\frac{3}{2u} + \frac{F'}{F} + 3\mathcal{W}' \right) \delta G_{xz}' + \frac{\omega^2}{4r_h^2 u^3 F^2} \delta G_{xz} = 0. \quad (\text{B5})$$

The solution to linear order in ω can again be found analytically and in the near-boundary region yields

$$\delta G_{xz} = \delta h_{xz}^z \left(1 + \frac{i\omega}{4r_h w^{3/2}} u^2 + \mathcal{O}(u^3) \right). \quad (\text{B6})$$

The relevant component of the stress-energy tensor is then

$$\langle T^{xz} \rangle = \frac{N_c^2}{2\pi^2} \left(\frac{i\omega r_h^3}{4w^{3/2}} \right) \delta h_{xz} + \dots, \quad (\text{B7})$$

which gives

$$\eta_{\parallel} = \frac{N_c^2}{2\pi^2} \left(\frac{r_h^3}{4w^{3/2}} \right) = \frac{1}{4\pi} \frac{v}{w} s, \quad (\text{B8})$$

as stated in Eq. (87).

(iii) *Resistivity* r_{\parallel}

The only equation of motion in this channel is

$$\delta B_{xy}'' + \left(\frac{3}{u} + \frac{F'}{F} - 2\mathcal{V}' + \mathcal{W}' \right) \delta B_{xy}' + \frac{\omega^2}{4r_h^2 u^3 F^2} \delta B_{xy} = 0, \quad (\text{B9})$$

which leads to the near-boundary solution

$$\delta B_{xy} = \delta B_{xy}^{(0)} \left(1 + \frac{i\omega v}{2r_h \sqrt{w}} \ln u + \mathcal{O}(u) \right). \quad (\text{B10})$$

The two-form current can then be written as

$$\langle \delta J^{xy} \rangle = \frac{2\pi^2}{N_c^2} \left(\frac{2i\omega v}{r_h \sqrt{w}} \right) \delta b_{xy} + \mathcal{O}(\omega^2), \quad (\text{B11})$$

which yields

$$r_{\parallel} = \frac{2\pi^2}{N_c^2} \left(\frac{v}{r_h \sqrt{w}} \right), \quad (\text{B12})$$

as stated in Eq. (87).

(iii) *Bulk viscosities* ζ_{\perp} , ζ_{\parallel} and ζ_{\times}

By counting the number of the relevant degrees of freedom, it turns out that there is only one dynamical mode in this decoupled system coming from $4 \times (2^{\text{nd}}\text{-order ODE's for } \delta g_{tt}, \delta g_{aa}, \delta g_{zz}, \delta b_{tz}) - 3 \times (1^{\text{st}}\text{-order ODE's for } \delta g_{tu}, \delta g_{uu}, \delta b_{zu})$. To find the dynamical mode, we start by solving the algebraic equations for δg_{tu} , δg_{uu} and δb_{zu} from the tu and uu components of Einstein's equation combined with the zu component of Maxwell's equations. Plugging these solutions into the four second-order equations involving δg_{tt} , δg_{aa} , δg_{zz} and δb_{tz} , we find that the remaining two non-trivial equations involve only δg_{aa} and δg_{zz} . The single resulting equation of motion can then be expressed in terms of the gauge-invariant variable $Z_s(u)$ defined as

$$Z_s(u) = \delta G^a_a - \frac{2\mathcal{V}'}{\mathcal{W}'} \delta G^z_z, \quad (\text{B13})$$

where $\delta g_{aa} = \delta g_{xx} + \delta g_{yy}$. The equation of motion for Z_s can be written

$$Z_s''(u) + C_1(\omega, u)Z_s'(u) + C_2(\omega, u)Z_s(u) = 0, \quad (\text{B14})$$

where

$$\begin{aligned} C_1 &= \frac{3}{2u} + \frac{F'}{F} + \frac{2\mathcal{W}''}{\mathcal{W}'} + 2\mathcal{V}' + \mathcal{W}' - 2 \left(\frac{2\mathcal{V}'' + \mathcal{W}''}{2\mathcal{V}' + \mathcal{W}'} \right), \\ C_2 &= -\frac{b^2 e^{-4\mathcal{V}}}{3u^3 F \mathcal{W}'} \left(\frac{F'}{F} + 4\mathcal{W}' \right) + \frac{\omega^2}{4r_h^2 u^3 F^2} - \frac{2F'^2}{3F^2 \mathcal{W}'} (\mathcal{V}' - \mathcal{W}') + \frac{4\mathcal{V}' F' (\mathcal{V}' - \mathcal{W}')^2}{3F \mathcal{W}' (2\mathcal{V}' + \mathcal{W}')} \\ &\quad + \frac{8\mathcal{V}'^2 (\mathcal{V}' + 2\mathcal{W}') (\mathcal{V}' - \mathcal{W}')}{2\mathcal{W}' (2\mathcal{V}' + \mathcal{W}')} . \end{aligned} \quad (\text{B15})$$

Now, suppose that the time-independent solution for Z_s is $\mathfrak{Z}^{(-)}$, so that $\mathfrak{Z}^{(-)}(u \rightarrow 0) = Z^{(0)} \equiv \delta h_{aa} - 2\delta h_{zz}$ (note that $\mathcal{V}'/\mathcal{W}' \rightarrow 1$ and $u \rightarrow 0$). The second solution, denoted as $\mathfrak{Z}^{(+)}$, contains the time-dependent information and can be found from the Wronskian

$$\mathfrak{Z}^{(+)}(u) = \mathfrak{Z}^{(-)}(u) \int_u^1 du' \frac{W_R(u')}{(\mathfrak{Z}^{(-)}(u'))^2}, \quad W_R = \left(\frac{2\mathcal{V}' + \mathcal{W}'}{\mathcal{W}'} \right)^2 \frac{e^{2\mathcal{V} + \mathcal{W}}}{u^{3/2} F}. \quad (\text{B16})$$

We then find that the near-boundary and near-horizon expansion for $\mathfrak{Z}^{(+)}$ are

$$\mathfrak{Z}^{(+)} = \begin{cases} \frac{9}{2v\sqrt{w}} \left[\mathfrak{Z}^{(-)}(0) \right]^{-1} u^2 + \mathcal{O}(u^3), & \text{near } u \rightarrow 0, \\ -9r_h \left(\frac{6+B^2}{6-B^2} \right)^2 \left[2\pi T \mathfrak{Z}^{(-)}(1) \right]^{-1} \ln(1-u) + \mathcal{O}(1-u), & \text{near } u \rightarrow 1. \end{cases} \quad (\text{B17})$$

The full solution is a linear combination, $Z_s(u) = \mathfrak{Z}^{(-)} + \alpha \mathfrak{Z}^{(+)}$, and the ingoing boundary condition sets the frequency-dependent function $\alpha(\omega)$ to be

$$\alpha(\omega) = \frac{i\omega}{2r_h} \left(\frac{(6+B^2)}{3(6-B^2)} \right)^2 \left[\mathfrak{Z}^{(-)}(1) \right]^2, \quad (\text{B18})$$

which allows us to write the solution for Z_s near the boundary as

$$Z_s = Z^{(0)} \left(1 + \frac{i\omega}{4r_h v \sqrt{w}} \left(\frac{6+B^2}{6-B^2} \right)^2 \left[\frac{\mathfrak{Z}^{(-)}(1)}{\mathfrak{Z}^{(-)}(0)} \right]^2 u^2 \right) + \dots \quad (\text{B19})$$

This expression can then be used to compute the bulk viscosities, for which we follow the approach by [87] and their analysis of the Green's function in the sound channel. In summary, we first find the expression for $\langle \delta T^{xx} + \delta T^{yy} \rangle$ and $\langle \delta T^{zz} \rangle$ in terms of δh_{tt} , δh_{aa} , δh_{zz} and δb_{tz} , and then relate the near-boundary data of the bulk modes δG_{tt} , δG_{aa} , δG_{zz} and δB_{tz} to those of Z_s . Then, we impose the radial gauge, $\delta G_{u\mu} = 0$ and $\delta B_{u\mu} = 0$, and solve the equations of motion near the boundary. The first-order equations of motion give the following relations:

$$\begin{aligned} h_{aa}^{(2)} + h_{tt}^{(2)} + h_{zz}^{(2)} + \frac{B^2 h_{aa}^{(0)}}{36v^2} &= 0, \\ 2 \left(h_{aa}^{(2)} + h_{zz}^{(2)} \right) + \frac{v_4^b}{v} \left(h_{aa}^{(0)} - 2h_{zz}^{(0)} \right) - f_4^b \left(h_{aa}^{(0)} + h_{zz}^{(0)} \right) &= 0. \end{aligned} \quad (\text{B20})$$

The coefficients $h_{\mu\nu}^{(n)}$ are defined through the near-boundary expansion of the metric fluctuation. By using the second-order dynamical equation and the radial gauge, the solutions are

$$\begin{aligned} \delta G_a^a &= h_{aa}^{(0)} + h_{aa}^{(2)} u^2 + \frac{h_{aa}^{(0)} B^2}{10v^2} u^2 \ln u + \mathcal{O}(\omega^2, u^3), \\ \delta G_t^t &= h_{tt}^{(0)} + h_{tt}^{(2)} u^2 - \frac{h_{aa}^{(0)} B^2}{20v^2} u^2 \ln u + \mathcal{O}(\omega^2, u^3), \\ \delta G_z^z &= h_{zz}^{(0)} + h_{zz}^{(2)} u^2 - \frac{h_{aa}^{(0)} B^2}{20v^2} u^2 \ln u + \mathcal{O}(\omega^2, u^3), \end{aligned} \quad (\text{B21})$$

where $h_{\mu\nu}^{(0)} \equiv \delta h_{\mu\nu}$ is the metric perturbation used throughout the paper. By combining Eqs. (B20) and (B21), and using the definition of the gauge-invariant mode Z_s , we find that

$$Z_s = Z^{(0)} + \frac{Z^{(0)} \omega^2}{6r_h^2} + Z^{(2)} u^2 + \frac{h_{aa}^{(0)} B^2}{5v^2} u^2 \ln u + \mathcal{O}(\omega^4), \quad (\text{B22})$$

where

$$Z^{(0)} = h_{aa}^{(0)} - 2h_{zz}^{(0)}, \quad Z^{(2)} = -3h_{zz}^{(2)} - \frac{v_4^b}{v} Z^{(0)} + f_4^b \left(h_{aa}^{(0)} + h_{zz}^{(0)} \right). \quad (\text{B23})$$

It is most convenient to extract the transport coefficients from $\langle \delta T^{zz} \rangle$:

$$\begin{aligned} \langle \delta T^{zz} \rangle &= -\frac{N_c^2 r_h^4 e^{2W}}{2\pi^2 w} \left(\frac{1}{2} \sqrt{uF} \left(\delta G_a^a + \delta G_t^t \right) + \left(\frac{3}{2u} + \frac{\sqrt{uF'}}{2F} + 2\sqrt{uF} \mathcal{V}' \right) \delta G_z^z \right) + \dots \\ &= \frac{N_c^2}{2\pi^2} r_h^4 h_{zz}^{(2)} + \dots \\ &= -\frac{N_c^2}{2\pi^2} \left(\frac{i\omega r_h^3}{12v\sqrt{w}} \left(\frac{6+B^2}{6-B^2} \right)^2 \left[\mathfrak{Z}^{(-)}(1)/\mathfrak{Z}^{(-)}(0) \right]^2 \right) (\delta h_{aa} - 2h_{zz}) + \dots \end{aligned}$$

Using the Kubo formula (A5), we find that

$$\begin{aligned} \zeta_{\parallel} &= \frac{N_c^2}{2\pi^2} \left(\frac{r_h^3}{3v\sqrt{w}} \left(\frac{6+B^2}{6-B^2} \right)^2 \left[\mathfrak{Z}^{(-)}(1)/\mathfrak{Z}^{(-)}(0) \right]^2 \right) \\ &= \frac{s}{4\pi} \left(\frac{4}{3} \left(\frac{6+B^2}{6-B^2} \right)^2 \left[\mathfrak{Z}^{(-)}(1)/\mathfrak{Z}^{(-)}(0) \right]^2 \right), \end{aligned} \quad (\text{B24})$$

and $\zeta_{\times}^{(2)} = -\zeta_{\parallel}/2$.

Similarly, we can extract ζ_{\perp} and $\zeta_{\times}^{(1)}$ from

$$\begin{aligned} \langle \delta T^{xx} \rangle + \langle \delta T^{yy} \rangle &= -\frac{N_c^2 r_h^4 e^{2\mathcal{V}}}{2\pi^2 v} \left[\frac{1}{2} \sqrt{uF} \left(\delta G_a^{a'} + \delta G_t^{t'} + \delta G_z^{z'} \right) \right. \\ &\quad \left. + \left(\frac{3}{2u} + \frac{\sqrt{uF'}}{2F} + \sqrt{uF}(\mathcal{V}' + \mathcal{W}') \right) \delta G_z^z \right] + \dots \\ &= \frac{N_c^2}{2\pi^2} \left(\frac{i\omega r_h^3}{12v\sqrt{w}} \left(\frac{6+B^2}{6-B^2} \right)^2 \left[\mathfrak{Z}^{(-)}(1)/\mathfrak{Z}^{(-)}(0) \right]^2 \right) (\delta h_{aa} - 2h_{zz}) + \dots, \end{aligned}$$

which gives $\zeta_{\perp} = \zeta_{\parallel}/4 = -\zeta_{\times}^{(1)}/2$. Hence, we find that $\zeta_{\times}^{(1)} = \zeta_{\times}^{(2)}$, which is the manifestation of the Onsager relation imposed in [22, 25]. This completes the derivation of expressions stated in Eq. (87).

As a simple check of our results, one can show that in the zero magnetic field limit,

$$\zeta_{\parallel} = -\lim_{\omega \rightarrow 0} \partial_{\omega} \text{Im} G_{TT}^{zz,zz}(\omega, 0) = -\frac{4}{3} \lim_{\omega \rightarrow 0} \partial_{\omega} \text{Im} G_{TT}^{xy,xy}(\omega, 0) = \frac{4}{3} \eta, \quad (\text{B25})$$

which is consistent with the fact that as $\mathcal{B} \rightarrow 0$, our plasma should become described by conformal hydrodynamics. By using standard relations between two-point functions in a neutral CFT fluid, (B25) is equivalent to the statement that bulk viscosity vanishes in conformal relativistic hydrodynamics (see e.g. [23]).²⁰ For another check, one can write the relation $\zeta_{\parallel} = 4\zeta_{\perp}$ in the language of two-point functions and obtain the relation $\lim_{\omega \rightarrow 0} [\partial_{\omega} G_{TT}^{aa,aa}(\omega, 0) - \frac{1}{2} \partial_{\omega} G_{TT}^{zz,zz}(\omega, 0)] = 0$, which is also satisfied by conformal relativistic hydrodynamics. Interestingly, this relation holds for all strengths of the magnetic field in the model studied in this work.

Appendix C: Dispersion relations of magnetosonic waves

In the magnetosonic channel, the polynomial equation in ω and k , which needs to be solved in order for us to find the dispersion relations $\omega(k)$ is a quartic equations in ω , which can be written in the following form:

$$\text{Det}[-i\omega \mathbf{1} + \mathbf{M}] = 0, \quad (\text{C1})$$

with $\mathbf{1}$ the 4×4 identity matrix and the non-zero components M_{ij} of the matrix \mathbf{M} given by

$$\begin{aligned} M_{11} &= r_{\perp} k^2 \sin^2 \theta \mathcal{A}_{11}, & M_{12} &= -r_{\perp} k^2 \mathcal{A}_{12}, & M_{13} &= ik \sin \theta \mathcal{A}_{13}, & M_{14} &= ik \frac{s \cos \theta}{\chi_{11}}, \\ M_{21} &= -r_{\perp} k^2 \sin^2 \theta \mathcal{A}_{21}, & M_{22} &= r_{\perp} k^2 \mathcal{A}_{22}, & M_{23} &= ik \rho \sin \theta, \\ M_{31} &= ik \sin \theta \mathcal{A}_{31}, & M_{32} &= ik \mathcal{A}_{32}, & M_{33} &= \mathcal{A}_{33} k^2, & \mathcal{M}_{34} &= \eta_{\perp} k^2 \mathcal{A}_{34}, \\ M_{41} &= i \frac{k}{T} \cos \theta, & M_{43} &= \eta_{\perp} k^2 \mathcal{A}_{43}, & M_{44} &= k^2 \mathcal{A}_{44}. \end{aligned} \quad (\text{C2})$$

²⁰ For a neutral relativistic fluid, one can show that $\text{Im} \langle \delta T^{xx} \rangle + \text{Im} \langle \delta T^{yy} \rangle = \omega \left(\frac{\eta}{3} + \zeta \right) \delta h_{aa} + \omega \left(\zeta - \frac{2}{3} \eta \right) \delta h_{zz} + \dots$, and that $\text{Im} \langle \delta T^{zz} \rangle = \frac{1}{2} \omega \left(\zeta - \frac{2}{3} \eta \right) \delta h_{aa} + \omega \left(\frac{2}{3} \eta + \frac{1}{2} \zeta \right) \delta h_{zz} + \dots$. In a conformal fluid with $\zeta = 0$, one therefore finds that $\lim_{\omega \rightarrow 0} \frac{1}{2} \partial_{\omega} \text{Im} G_{TT}^{aa,aa}(\omega, 0) = \lim_{\omega \rightarrow 0} \frac{1}{4} \partial_{\omega} \text{Im} G_{TT}^{zz,zz}(\omega, 0) = -\eta/3$. The relation $\zeta_{\perp} = \zeta_{\parallel}/4$ came equations $\lim_{\omega \rightarrow 0} \partial_{\omega} \text{Im} G_{TT}^{aa,aa}(\omega, 0) = -2\zeta_{\perp}$ and $\lim_{\omega \rightarrow 0} \partial_{\omega} \text{Im} G_{TT}^{zz,zz}(\omega, 0) = -\zeta_{\parallel}$ (see Eq. (A5)).

The coefficients \mathcal{A}_{ij} are

$$\begin{aligned}
\mathcal{A}_{11} &= \frac{1}{2T^2\chi_{11}}(\mu + T\chi_{12})(\mu - T\mu_{21}), & \mathcal{A}_{12} &= \frac{1}{2T\rho\chi_{11}}(\mu + T\chi_{12})(\mu \cos^2\theta + \rho\chi_{22} \sin^2\theta), \\
\mathcal{A}_{13} &= \frac{s - \rho\chi_{12}}{\chi_{11}}, & \mathcal{A}_{21} &= \frac{\mu - T\chi_{21}}{2T}, \\
\mathcal{A}_{22} &= \frac{1}{2\rho}(\mu \cos^2\theta + \rho\chi_{22} \sin^2\theta), & \mathcal{A}_{31} &= \frac{s + \rho\chi_{21}}{\varepsilon + p}, \\
\mathcal{A}_{32} &= \frac{2\rho}{(\varepsilon + p) \sin\theta} \mathcal{A}_{22}, & \mathcal{A}_{33} &= \left(\frac{\eta_{\parallel} \cos^2\theta + (\eta_{\perp} + \zeta_{\perp}) \sin^2\theta}{\varepsilon + p} \right), \\
\mathcal{A}_{34} &= \frac{\cos\theta \sin\theta}{\varepsilon + p}, & \mathcal{A}_{43} &= \frac{\varepsilon + p}{sT} \mathcal{A}_{34}, \\
\mathcal{A}_{44} &= \frac{2\zeta_{\parallel} \cos^2\theta + \eta_{\parallel} \sin^2\theta}{sT}.
\end{aligned} \tag{C3}$$

By computing the determinant in (C1), the resulting quartic equation is

$$\omega^4 + c_3\omega^3 + c_2\omega^2 + c_1\omega + c_0 = 0, \tag{C4}$$

where c_i are functions of thermodynamics quantities, transport coefficients, k and θ . The expressions for c_i in terms of \mathcal{A}_{ij} in (C3) are

$$\begin{aligned}
c_3 &= ik^2 (\mathcal{A}_{33} + \mathcal{A}_{44} + A_{22}r_{\perp} + A_{11}r_{\perp} \sin^2\theta), \\
c_2 &= -\frac{k^2}{T\chi_{11}} (s \cos^2\theta + T\chi_{11} \sin\theta(\mathcal{A}_{32}\rho + \mathcal{A}_{13}\mathcal{A}_{31} \sin\theta)) - k^4 \left[\mathcal{A}_{22}\mathcal{A}_{44}r_{\perp} + \mathcal{A}_{33}(\mathcal{A}_{44} + A_{22}r_{\perp}) \right. \\
&\quad \left. - \mathcal{A}_{34}\eta_{\perp}^2 + r_{\perp} (A_{11}(\mathcal{A}_{33} + \mathcal{A}_{44}) + r_{\perp} \sin^2\theta(A_{11}\mathcal{A}_{22} - A_{12}\mathcal{A}_{21})) \right], \\
c_1 &= -i \frac{k^4}{T\chi_{11}} \left\{ s(r_{\perp}\mathcal{A}_{22} + \mathcal{A}_{33}) \cos^2\theta - \eta_{\perp} \cos\theta \sin\theta (sT\mathcal{A}_{31} + \chi_{11}\mathcal{A}_{13}\mathcal{A}_{34}) + \chi_{11}T \sin\theta \left[\rho\mathcal{A}_{32}\mathcal{A}_{44} \right. \right. \\
&\quad \left. \left. + \mathcal{A}_{31} \sin\theta (\mathcal{A}_{13}\mathcal{A}_{44} + r_{\perp}\mathcal{A}_{13}\mathcal{A}_{22} + r_{\perp}\rho\mathcal{A}_{12}) + r_{\perp}\mathcal{A}_{32} \sin^2\theta (\mathcal{A}_{13}\mathcal{A}_{21} + \rho\mathcal{A}_{11}) \right] \right\} \\
&\quad - ir_{\perp}k^6 \left\{ \mathcal{A}_{22}(\mathcal{A}_{33}\mathcal{A}_{44} - \mathcal{A}_{34}\eta_{\perp}^2) + \sin^2\theta \left[-r_{\perp}\mathcal{A}_{12}\mathcal{A}_{21}(\mathcal{A}_{33} + \mathcal{A}_{44}) \right. \right. \\
&\quad \left. \left. + \mathcal{A}_{11} \sin^2\theta (\mathcal{A}_{33}\mathcal{A}_{44} + r_{\perp}\mathcal{A}_{22}\mathcal{A}_{33} + r_{\perp}\mathcal{A}_{22}\mathcal{A}_{44} - \eta_{\perp}^2\mathcal{A}_{34}) \right] \right\}, \\
c_0 &= \left(\frac{s\rho\mathcal{A}_{23} \cos^2\theta \sin^2\theta}{T\chi_{11}} \right) k^4 + \frac{r_{\perp}k^6}{T\chi_{11}} \left\{ s\mathcal{A}_{22}\mathcal{A}_{33} \cos^2\theta + \chi_{11}\mathcal{A}_{32}\mathcal{A}_{44}(\mathcal{A}_{13}\mathcal{A}_{21} + \rho\mathcal{A}_{11}) \sin^3\theta \right. \\
&\quad \left. + \chi_{11}\mathcal{A}_{13}\mathcal{A}_{31}\mathcal{A}_{44}(\mathcal{A}_{13}\mathcal{A}_{22} + \rho\mathcal{A}_{12}) + \eta_{\perp} \cos\theta \sin\theta \left[sT\mathcal{A}_{22}\mathcal{A}_{31} + \chi_{11}\mathcal{A}_{13}\mathcal{A}_{22}\mathcal{A}_{34} \right. \right. \\
&\quad \left. \left. + \chi_{11}\rho\mathcal{A}_{12}\mathcal{A}_{34} + sT\mathcal{A}_{21}\mathcal{A}_{32} \sin\theta \right] \right\} + r_{\perp}^2 (\mathcal{A}_{12}\mathcal{A}_{21} - \mathcal{A}_{11}\mathcal{A}_{22})(\mathcal{A}_{33}\mathcal{A}_{34}\eta_{\perp}^2) k^8 \sin^2\theta.
\end{aligned} \tag{C5}$$

In principle, Eq. (C4) gives a closed-form solution for the four $\omega(k)$. In practice, the explicit solutions are extremely lengthy so it is often more convenient to find the roots of (C4) numerically

(our equations of state and transport coefficients are in any case given numerically), or by using various expansions, e.g. small k/T or small $k/\sqrt{\mathcal{B}}$.

-
- [1] Paul M Bellan, *Fundamentals of plasma physics* (Cambridge University Press, 2008).
 - [2] Jeffrey P. Freidberg, *Ideal MHD*: (Cambridge University Press, Cambridge, 2014).
 - [3] Sergei Dubovsky, Lam Hui, Alberto Nicolis, and Dam Thanh Son, “Effective field theory for hydrodynamics: thermodynamics, and the derivative expansion,” *Phys. Rev.* **D85**, 085029 (2012), [arXiv:1107.0731 \[hep-th\]](#).
 - [4] Solomon Endlich, Alberto Nicolis, Rafael A. Porto, and Junpu Wang, “Dissipation in the effective field theory for hydrodynamics: First order effects,” *Phys. Rev.* **D88**, 105001 (2013), [arXiv:1211.6461 \[hep-th\]](#).
 - [5] Sašo Grozdanov and Janos Polonyi, “Viscosity and dissipative hydrodynamics from effective field theory,” *Phys. Rev.* **D91**, 105031 (2015), [arXiv:1305.3670 \[hep-th\]](#).
 - [6] Alberto Nicolis, Riccardo Penco, and Rachel A. Rosen, “Relativistic Fluids, Superfluids, Solids and Supersolids from a Coset Construction,” *Phys. Rev.* **D89**, 045002 (2014), [arXiv:1307.0517 \[hep-th\]](#).
 - [7] Pavel Kovtun, Guy D. Moore, and Paul Romatschke, “Towards an effective action for relativistic dissipative hydrodynamics,” *JHEP* **07**, 123 (2014), [arXiv:1405.3967 \[hep-ph\]](#).
 - [8] Michael Harder, Pavel Kovtun, and Adam Ritz, “On thermal fluctuations and the generating functional in relativistic hydrodynamics,” *JHEP* **07**, 025 (2015), [arXiv:1502.03076 \[hep-th\]](#).
 - [9] Sašo Grozdanov and Janos Polonyi, “Dynamics of the electric current in an ideal electron gas: A sound mode inside the quasiparticles,” *Phys. Rev.* **D92**, 065009 (2015), [arXiv:1501.06620 \[hep-th\]](#).
 - [10] Michael Crossley, Paolo Glorioso, and Hong Liu, “Effective field theory of dissipative fluids,” (2015), [arXiv:1511.03646 \[hep-th\]](#).
 - [11] Paolo Glorioso, Michael Crossley, and Hong Liu, “Effective field theory for dissipative fluids (II): classical limit, dynamical KMS symmetry and entropy current,” (2017), [arXiv:1701.07817 \[hep-th\]](#).
 - [12] Felix M. Haehl, R. Loganayagam, and Mukund Rangamani, “The Fluid Manifesto: Emergent symmetries, hydrodynamics, and black holes,” *JHEP* **01**, 184 (2016), [arXiv:1510.02494 \[hep-th\]](#).
 - [13] Felix M. Haehl, R. Loganayagam, and M. Rangamani, “Topological sigma models & dissipative hydrodynamics,” *JHEP* **04**, 039 (2016), [arXiv:1511.07809 \[hep-th\]](#).
 - [14] David Montenegro and Giorgio Torrieri, “Lagrangian formulation of relativistic Israel-Stewart hydrodynamics,” *Phys. Rev.* **D94**, 065042 (2016), [arXiv:1604.05291 \[hep-th\]](#).
 - [15] Paolo Glorioso and Hong Liu, “The second law of thermodynamics from symmetry and unitarity,” (2016), [arXiv:1612.07705 \[hep-th\]](#).
 - [16] Ping Gao and Hong Liu, “Emergent Supersymmetry in Local Equilibrium Systems,” (2017), [arXiv:1701.07445 \[hep-th\]](#).
 - [17] Kristan Jensen, Natalia Pinzani-Fokeeva, and Amos Yarom, “Dissipative hydrodynamics in superspace,” (2017), [arXiv:1701.07436 \[hep-th\]](#).
 - [18] Rudolf Baier, Paul Romatschke, Dam Thanh Son, Andrei O. Starinets, and Mikhail A. Stephanov, “Relativistic viscous hydrodynamics, conformal invariance, and holography,” *JHEP* **04**, 100 (2008), [arXiv:0712.2451 \[hep-th\]](#).
 - [19] Sayantani Bhattacharyya, Veronika E Hubeny, Shiraz Minwalla, and Mukund Rangamani, “Nonlinear Fluid Dynamics from Gravity,” *JHEP* **02**, 045 (2008), [arXiv:0712.2456 \[hep-th\]](#).
 - [20] Paul Romatschke, “Relativistic Viscous Fluid Dynamics and Non-Equilibrium Entropy,” *Class. Quant. Grav.* **27**, 025006 (2010), [arXiv:0906.4787 \[hep-th\]](#).

- [21] Sašo Grozdanov and Nikolaos Kaplis, “Constructing higher-order hydrodynamics: The third order,” *Phys. Rev.* **D93**, 066012 (2016), [arXiv:1507.02461 \[hep-th\]](#).
- [22] Sašo Grozdanov, Diego M. Hofman, and Nabil Iqbal, “Generalized global symmetries and dissipative magnetohydrodynamics,” *Phys. Rev.* **D95**, 096003 (2017), [arXiv:1610.07392 \[hep-th\]](#).
- [23] Pavel Kovtun, “Lectures on hydrodynamic fluctuations in relativistic theories,” *INT Summer School on Applications of String Theory Seattle, Washington, USA, July 18-29, 2011*, *J. Phys.* **A45**, 473001 (2012), [arXiv:1205.5040 \[hep-th\]](#).
- [24] Daniel Schubring, “Dissipative String Fluids,” *Phys. Rev.* **D91**, 043518 (2015), [arXiv:1412.3135 \[hep-th\]](#).
- [25] Juan Hernandez and Pavel Kovtun, “Relativistic magnetohydrodynamics,” (2017), [arXiv:1703.08757 \[hep-th\]](#).
- [26] Xu-Guang Huang, Armen Sedrakian, and Dirk H. Rischke, “Kubo formulae for relativistic fluids in strong magnetic fields,” *Annals Phys.* **326**, 3075–3094 (2011), [arXiv:1108.0602 \[astro-ph.HE\]](#).
- [27] R. Critelli, S. I. Finazzo, M. Zaniboni, and J. Noronha, “Anisotropic shear viscosity of a strongly coupled non-Abelian plasma from magnetic branes,” *Phys. Rev.* **D90**, 066006 (2014), [arXiv:1406.6019 \[hep-th\]](#).
- [28] Stefano Ivo Finazzo, Renato Critelli, Romulo Rougemont, and Jorge Noronha, “Momentum transport in strongly coupled anisotropic plasmas in the presence of strong magnetic fields,” *Phys. Rev.* **D94**, 054020 (2016), [arXiv:1605.06061 \[hep-ph\]](#).
- [29] Pavel Kovtun, “Thermodynamics of polarized relativistic matter,” *JHEP* **07**, 028 (2016), [arXiv:1606.01226 \[hep-th\]](#).
- [30] David Montenegro, Leonardo Tinti, and Giorgio Torrieri, “The ideal relativistic fluid limit for a medium with polarization,” (2017), [arXiv:1701.08263 \[hep-th\]](#).
- [31] Davide Gaiotto, Anton Kapustin, Nathan Seiberg, and Brian Willett, “Generalized Global Symmetries,” *JHEP* **02**, 172 (2015), [arXiv:1412.5148 \[hep-th\]](#).
- [32] G. Policastro, Dan T. Son, and Andrei O. Starinets, “The Shear viscosity of strongly coupled N=4 supersymmetric Yang-Mills plasma,” *Phys. Rev. Lett.* **87**, 081601 (2001), [arXiv:hep-th/0104066 \[hep-th\]](#).
- [33] Giuseppe Policastro, Dam T. Son, and Andrei O. Starinets, “From AdS / CFT correspondence to hydrodynamics,” *JHEP* **09**, 043 (2002), [arXiv:hep-th/0205052 \[hep-th\]](#).
- [34] Giuseppe Policastro, Dam T. Son, and Andrei O. Starinets, “From AdS / CFT correspondence to hydrodynamics. 2. Sound waves,” *JHEP* **12**, 054 (2002), [arXiv:hep-th/0210220 \[hep-th\]](#).
- [35] Diego M. Hofman and Nabil Iqbal, “Generalized global symmetries and holography,” To appear.
- [36] John F. Fuini and Laurence G. Yaffe, “Far-from-equilibrium dynamics of a strongly coupled non-Abelian plasma with non-zero charge density or external magnetic field,” *JHEP* **07**, 116 (2015), [arXiv:1503.07148 \[hep-th\]](#).
- [37] Steven Weinberg, *The Quantum Theory of Fields. Vol. 1: Foundations* (Cambridge University Press, 2005).
- [38] Steven Weinberg, *The Quantum Theory of Fields. Vol. 2: Modern Applications* (Cambridge University Press, 2013).
- [39] Michael E. Peskin and Daniel V. Schroeder, *An Introduction to quantum field theory* (1995).
- [40] Daisuke Yamada and Laurence G. Yaffe, “Phase diagram of N=4 super-Yang-Mills theory with R-symmetry chemical potentials,” *JHEP* **09**, 027 (2006), [arXiv:hep-th/0602074 \[hep-th\]](#).
- [41] Aleksey Cherman, Sašo Grozdanov, and Edward Hardy, “Searching for Fermi Surfaces in Super-QED,” *JHEP* **06**, 046 (2014), [arXiv:1308.0335 \[hep-th\]](#).

- [42] Daniel Z. Freedman, Samir D. Mathur, Alec Matusis, and Leonardo Rastelli, “Correlation functions in the CFT(d) / AdS(d+1) correspondence,” *Nucl. Phys.* **B546**, 96–118 (1999), [arXiv:hep-th/9804058 \[hep-th\]](#).
- [43] D. Anselmi, J. Erlich, D. Z. Freedman, and A. A. Johansen, “Positivity constraints on anomalies in supersymmetric gauge theories,” *Phys. Rev.* **D57**, 7570–7588 (1998), [arXiv:hep-th/9711035 \[hep-th\]](#).
- [44] Eric D’Hoker and Per Kraus, “Magnetic Brane Solutions in AdS,” *JHEP* **10**, 088 (2009), [arXiv:0908.3875 \[hep-th\]](#).
- [45] Stefan Janiszewski and Matthias Kaminski, “Quasinormal modes of magnetic and electric black branes versus far from equilibrium anisotropic fluids,” *Phys. Rev.* **D93**, 025006 (2016), [arXiv:1508.06993 \[hep-th\]](#).
- [46] Martin Ammon, Matthias Kaminski, Roshan Koirala, Julian Leiber, and Jackson Wu, “Quasinormal modes of charged magnetic black branes & chiral magnetic transport,” *JHEP* **04**, 067 (2017), [arXiv:1701.05565 \[hep-th\]](#).
- [47] Donald Marolf and Simon F. Ross, “Boundary Conditions and New Dualities: Vector Fields in AdS/CFT,” *JHEP* **0611**, 085 (2006), [arXiv:hep-th/0606113 \[hep-th\]](#).
- [48] Niko Jokela, Gilad Lifschytz, and Matthew Lippert, “Holographic anyonic superfluidity,” *JHEP* **10**, 014 (2013), [arXiv:1307.6336 \[hep-th\]](#).
- [49] Elli Pomoni and Leonardo Rastelli, “Large N Field Theory and AdS Tachyons,” *JHEP* **04**, 020 (2009), [arXiv:0805.2261 \[hep-th\]](#).
- [50] Idse Heemskerck and Joseph Polchinski, “Holographic and Wilsonian Renormalization Groups,” *JHEP* **06**, 031 (2011), [arXiv:1010.1264 \[hep-th\]](#).
- [51] Thomas Faulkner, Hong Liu, and Mukund Rangamani, “Integrating out geometry: Holographic Wilsonian RG and the membrane paradigm,” *JHEP* **08**, 051 (2011), [arXiv:1010.4036 \[hep-th\]](#).
- [52] Saso Grozdanov, “Wilsonian Renormalisation and the Exact Cut-Off Scale from Holographic Duality,” *JHEP* **06**, 079 (2012), [arXiv:1112.3356 \[hep-th\]](#).
- [53] Thomas Faulkner and Nabil Iqbal, “Friedel oscillations and horizon charge in 1D holographic liquids,” *JHEP* **07**, 060 (2013), [arXiv:1207.4208 \[hep-th\]](#).
- [54] Steven S. Gubser, “AdS / CFT and gravity,” *Phys. Rev.* **D63**, 084017 (2001), [arXiv:hep-th/9912001 \[hep-th\]](#).
- [55] Eric D’Hoker and Per Kraus, “Charged Magnetic Brane Solutions in AdS (5) and the fate of the third law of thermodynamics,” *JHEP* **03**, 095 (2010), [arXiv:0911.4518 \[hep-th\]](#).
- [56] Nabil Iqbal and Hong Liu, “Universality of the hydrodynamic limit in AdS/CFT and the membrane paradigm,” *Phys. Rev.* **D79**, 025023 (2009), [arXiv:0809.3808 \[hep-th\]](#).
- [57] Steven S. Gubser, Silviu S. Pufu, and Fabio D. Rocha, “Bulk viscosity of strongly coupled plasmas with holographic duals,” *JHEP* **08**, 085 (2008), [arXiv:0806.0407 \[hep-th\]](#).
- [58] Omid Saremi and Dam Thanh Son, “Hall viscosity from gauge/gravity duality,” *JHEP* **04**, 091 (2012), [arXiv:1103.4851 \[hep-th\]](#).
- [59] Aristomenis Donos and Jerome P. Gauntlett, “Thermoelectric DC conductivities from black hole horizons,” *JHEP* **11**, 081 (2014), [arXiv:1406.4742 \[hep-th\]](#).
- [60] Elliot Banks, Aristomenis Donos, and Jerome P. Gauntlett, “Thermoelectric DC conductivities and Stokes flows on black hole horizons,” *JHEP* **10**, 103 (2015), [arXiv:1507.00234 \[hep-th\]](#).
- [61] Richard A. Davison, Blaise Goutéraux, and Sean A. Hartnoll, “Incoherent transport in clean quantum critical metals,” *JHEP* **10**, 112 (2015), [arXiv:1507.07137 \[hep-th\]](#).
- [62] Umut Gursoy and Javier Tarrio, “Horizon universality and anomalous conductivities,” *JHEP* **10**, 058 (2015), [arXiv:1410.1306 \[hep-th\]](#).

- [63] Sašo Grozdanov and Napat Poovuttikul, “Universality of anomalous conductivities in theories with higher-derivative holographic duals,” *JHEP* **09**, 046 (2016), [arXiv:1603.08770 \[hep-th\]](#).
- [64] Sebastian de Haro, Sergey N. Solodukhin, and Kostas Skenderis, “Holographic reconstruction of space-time and renormalization in the AdS / CFT correspondence,” *Commun. Math. Phys.* **217**, 595–622 (2001), [arXiv:hep-th/0002230 \[hep-th\]](#).
- [65] Marika Taylor, “More on counterterms in the gravitational action and anomalies,” (2000), [arXiv:hep-th/0002125 \[hep-th\]](#).
- [66] José M. Martín-García, “xAct: Efficient Tensor Computer Algebra, <http://www.xact.es/>,”.
- [67] Frederik Denef, Sean A. Hartnoll, and Subir Sachdev, “Quantum oscillations and black hole ringing,” *Phys. Rev.* **D80**, 126016 (2009), [arXiv:0908.1788 \[hep-th\]](#).
- [68] Frederik Denef, Sean A. Hartnoll, and Subir Sachdev, “Black hole determinants and quasinormal modes,” *Class. Quant. Grav.* **27**, 125001 (2010), [arXiv:0908.2657 \[hep-th\]](#).
- [69] Simon Caron-Huot and Omid Saremi, “Hydrodynamic Long-Time tails From Anti de Sitter Space,” *JHEP* **11**, 013 (2010), [arXiv:0909.4525 \[hep-th\]](#).
- [70] Stefan A. Stricker, “Holographic thermalization in N=4 Super Yang-Mills theory at finite coupling,” *Eur. Phys. J.* **C74**, 2727 (2014), [arXiv:1307.2736 \[hep-th\]](#).
- [71] Sebastian Waeber, Andreas Schaefer, Alekski Vuorinen, and Laurence G. Yaffe, “Finite coupling corrections to holographic predictions for hot QCD,” *JHEP* **11**, 087 (2015), [arXiv:1509.02983 \[hep-th\]](#).
- [72] Sašo Grozdanov, Nikolaos Kaplis, and Andrei O. Starinets, “From strong to weak coupling in holographic models of thermalization,” *JHEP* **07**, 151 (2016), [arXiv:1605.02173 \[hep-th\]](#).
- [73] Sašo Grozdanov and Wilke van der Schee, “Coupling constant corrections in holographic heavy ion collisions,” (2016), [arXiv:1610.08976 \[hep-th\]](#).
- [74] Sašo Grozdanov and Andrei O. Starinets, “Second-order transport, quasinormal modes and zero-viscosity limit in the Gauss-Bonnet holographic fluid,” *JHEP* **03**, 166 (2017), [arXiv:1611.07053 \[hep-th\]](#).
- [75] Dam T. Son and Andrei O. Starinets, “Minkowski space correlators in AdS / CFT correspondence: Recipe and applications,” *JHEP* **09**, 042 (2002), [arXiv:hep-th/0205051 \[hep-th\]](#).
- [76] C. P. Herzog and D. T. Son, “Schwinger-Keldysh propagators from AdS/CFT correspondence,” *JHEP* **03**, 046 (2003), [arXiv:hep-th/0212072 \[hep-th\]](#).
- [77] V. E. Fortov and V. B. Mintsev, “Quantum bound of the shear viscosity of a strongly coupled plasma,” *Phys. Rev. Lett.* **111**, 125004 (2013).
- [78] Sašo Grozdanov, Andrew Lucas, Subir Sachdev, and Koenraad Schalm, “Absence of disorder-driven metal-insulator transitions in simple holographic models,” *Phys. Rev. Lett.* **115**, 221601 (2015), [arXiv:1507.00003 \[hep-th\]](#).
- [79] Andrew Lucas and Sean A. Hartnoll, “Resistivity bound for hydrodynamic bad metals,” (2017), [arXiv:1704.07384 \[cond-mat.str-el\]](#).
- [80] L. P. Kadanoff and P. C. Martin, “Hydrodynamic equations and correlation functions,” *Annals of Physics* **24**, 419–469 (1963).
- [81] Aleksey Cherman, Thomas D. Cohen, and Abhinav Nellore, “A Bound on the speed of sound from holography,” *Phys. Rev.* **D80**, 066003 (2009), [arXiv:0905.0903 \[hep-th\]](#).
- [82] Aleksey Cherman and Abhinav Nellore, “Universal relations of transport coefficients from holography,” *Phys. Rev.* **D80**, 066006 (2009), [arXiv:0905.2969 \[hep-th\]](#).
- [83] Paul M. Hohler and Mikhail A. Stephanov, “Holography and the speed of sound at high temperatures,” *Phys. Rev.* **D80**, 066002 (2009), [arXiv:0905.0900 \[hep-th\]](#).
- [84] Carlos Hoyos, Niko Jokela, David Rodríguez Fernández, and Alekski Vuorinen, “Breaking the sound barrier in AdS/CFT,” *Phys. Rev.* **D94**, 106008 (2016), [arXiv:1609.03480 \[hep-th\]](#).

- [85] Sašo Grozdanov and Andrei O. Starinets, “On the universal identity in second order hydrodynamics,” *JHEP* **03**, 007 (2015), [arXiv:1412.5685 \[hep-th\]](#).
- [86] Felix M. Haehl, R. Loganayagam, and Mukund Rangamani, “Adiabatic hydrodynamics: The eightfold way to dissipation,” *JHEP* **05**, 060 (2015), [arXiv:1502.00636 \[hep-th\]](#).
- [87] Mohammad Edalati, Juan I. Jottar, and Robert G. Leigh, “Holography and the sound of criticality,” *JHEP* **10**, 058 (2010), [arXiv:1005.4075 \[hep-th\]](#).